AFWAL-TR-82-3031

INTRODUCTION TO COMPUTATIONAL AERODYNAMICS

W. L. Hankey

Computational Aerodynamics Group
Aeromechanics Division

April 1983

Final Report for 5 January - 3 July 1981

Approved for public release; distribution unlimited.

FLIGHT DYNAMICS LABORATORY
AIR FORCE WRIGHT AERONAUTICAL LABORATORIES
AIR FORCE SYSTEMS COMMAND
WRIGHT-PATTERSON AIR FORCE BASE, OHIO 45433

NOTICE

When Government drawings, specifications, or other data are used for any purpose other than in connection with a definitely related Government procurement operation, the United States Government thereby incurs no responsibility nor any obligation whatsoever; and the fact that the government may have formulated, furnished, or in any way supplied the said drawings, specifications, or other data, is not to be regarded by implication or otherwise as in any manner licensing the holder or any other person or corporation, or conveying any rights or permission to manufacture use, or sell any patented invention that may in any way be related thereto.

This report has been reviewed by the Office of Public Affairs (ASD/PA) and is releasable to the National Technical Information Service (NTIS). At NTIS, it will be available to the general public, including foreign nations.

This technical report has been reviewed and is approved for publication.

PROJECT ENGINEER

LOWELL C. KEEL, Lt Col, USAF
Chief, Aerodynamics & Airframe Branch

FOR THE COMMANDER

JOHN R. CHEVALIER, Colonel, USAF
Chief, Aeromechanics Division

"If your address has changed, if you wish to be removed from our mailing list, or if the addressee is no longer employed by your organization please notify AFWAL/FIMM, *W-PAFB, OH 45433 to help us maintain a current mailing list".*

Copies of this report should not be returned unless return is required by security considerations, contractual obligations, or notice on a specific document.

REPORT DOCUMENTATION PAGE		READ INSTRUCTIONS BEFORE COMPLETING FORM
1. REPORT NUMBER AFWAL-TR-82-3031	2. GOVT ACCESSION NO.	3. RECIPIENT'S CATALOG NUMBER
4. TITLE (and Subtitle) INTRODUCTION TO COMPUTATIONAL AERODYNAMICS		5. TYPE OF REPORT & PERIOD COVERED Final Report 6. PERFORMING ORG. REPORT NUMBER
7. AUTHOR(s) W. L. Hankey		8. CONTRACT OR GRANT NUMBER(s)
9. PERFORMING ORGANIZATION NAME AND ADDRESS Flight Dynamics Laboratory (AFWAL/FIMM) Air Force Wright Aeronautical Laboratories Wright-Patterson AFB, OH 45433		10. PROGRAM ELEMENT, PROJECT, TASK AREA & WORK UNIT NUMBERS 2307N606
11. CONTROLLING OFFICE NAME AND ADDRESS Flight Dynamics Laboratory (AFWAL/FIM) Air Force Wright Aeronautical Laboratories Wright-Patterson AFB, OH 45433		12. REPORT DATE April 198? 13. NUMBER OF PAGES 124
14. MONITORING AGENCY NAME & ADDRESS(if different from Controlling Office)		15. SECURITY CLASS. (of this report) UNCLASSIFIED 15a. DECLASSIFICATION/DOWNGRADING SCHEDULE

16. DISTRIBUTION STATEMENT (of this Report)

Approved for public release; distribution unlimited.

17. DISTRIBUTION STATEMENT (of the abstract entered in Block 20, if different from Report)

18. SUPPLEMENTARY NOTES

19. KEY WORDS (Continue on reverse side if necessary and identify by block number)
Computational Fluid Dynamics
Numerical Methods
Navier-Stokes Solutions

20. ABSTRACT (Continue on reverse side if necessary and identify by block number)

During the last decade remarkable advances have occurred in our ability to solve the Navier-Stokes equations for complex flows. Algorithms were developed and the speed and capacity of digital computers evolved to permit these advances. This report traces some of the significant features of this new field of Computational Fluid Dynamics (CFD). The objective is to provide an introduction to CFD for engineers starting in the field. The governing equations are first derived in the divergence form currently in use. The use of numerical methods is first demonstrated by solving the boundary layer equations. (Cont'd)

20. ABSTRACT (Cont'd)

Stability and accuracy are then discussed. Several popular algorithms for solving partial differential equations by finite differences are presented. The shock wave structure is then solved by means of one of these algorithms. Numerical techniques for grid generation are discussed along with the general transformation procedure. Self-excited fluid dynamic oscillations encountered in CFD are addressed. It is hoped that by studying these specific topics an engineer can become functional in the field of CFD. This report has been used to assist in teaching AE 7.51 (CFD) at the Air Force Institute of Technology, WPAFB, Ohio.

FOREWORD

This report is a review of the fundamental procedures developed for solving practical USAF problems by means of Computational Fluid Dynamic techniques. It represents the efforts of the Computational Aerodynamics Group over a several year period, directed by Dr. Wilbur L. Hankey under project 2307N603.

TABLE OF CONTENTS

SECTION		PAGE
I	HISTORICAL BACKGROUND	1
II	GOVERNING EQUATIONS IN AERODYNAMICS	3
	1. Vector Analysis	3
	2. Derivation of Navier-Stokes Equations	4
	3. Continuity	5
	4. Momentum Equation	5
	5. Energy Equation	6
	6. Divergence Form of Equations	7
III	SURVEY OF AERODYNAMIC PREDICTION METHODS	11
	1. Level III. Navier-Stokes	11
	a. Level III.A. Parabolized Navier-Stokes	11
	b. Level III.B. Two-D Boundary Layer	11
	2. Level II	12
	a. Level II.A. Inviscid (Euler)	12
	b. Level II.B. Inviscid, Irrotational (Full Potential)	13
	3. Level I. Linearized Equation	14
IV	ANALYTIC SOLUTION OF BOUNDARY LAYERS	18
V	NUMERICAL SOLUTION OF BOUNDARY LAYERS	21
	1. Summary of Numerical Procedure for Boundary Layer Calculations	27
VI	TRUNCATION ERROR ANALYSIS	28
	1. Richardson's Extrapolation	29
VII	STABILITY ANALYSIS	31
	1. Model Equations	31
	2. Von Neumann Stability Analysis	32
	3. Summary	34

SECTION		PAGE
	4. Eigenvalue Interpretation of Gain	34
	5. Diffusion Equation	34
VIII	NUMERICAL ALGORITHMS	36
	1. Explicit Methods	36
	2. Midpoint Leapfrog Method	36
	3. MacCormack Explicit Method	38
	4. Fully Implicit	39
	5. Crank Nicolson Implicit	40
IX	SHOCK WAVE STRUCTURE	42
	1. Analytic Solution	43
	2. Summary of Five Boundary Conditions	45
	3. Numerical Solution	45
	4. Five Boundary Conditions	46
X	ARTIFICIAL VISCOSITY	47
	1. Normal Stress Damping	49
	2. Von Neumann Richtmyer Damping	49
	3. MacCormack's Pressure Damping	50
	4. Upwind Differencing	50
XI	COORDINATE TRANSFORMATION PROCEDURE	52
	1. Body-Oriented Coordinates	52
	2. Clustering of Grid Points	55
	3. Summary	57
XII	PARABOLIZED NAVIER-STOKES	59
XIII	AIR PROPERTIES	65
	1. Thermodynamic Properties	65
	2. Real Gas Effects	66
	3. Transport Properties	68

SECTION		PAGE
XIV	BOUNDARY CONDITIONS	71
	1. Surface Boundary Conditions	71
	2. Far Field Boundary Conditions	75
	3. Summary One-Dimensional Flow	79
	4. Branch Cut Boundary Conditions	83
	5. Symmetry Plane	83
	6. Periodic Conditions	83
	7. Classification of Partial Differential Equations	83
XV	GRID GENERATION PROCEDURE	87
	1. Algebraic Method	87
	2. Elliptic Method	88
	3. SOR Solver	90
	4. Alternating Direction Implicit (ADI) Solver	91
	5. Hyperbolic Method	91
XVI	FLUID DYNAMIC STABILITY	96
	1. Parallel Flow	96
	2. Condition for Instability	98
XVII	TURBULENCE MODELS	100
	1. Evaluation of Eddy Viscosity	103
	2. Boussinesq Model	103
	3. Clauser Law of the Wake	103
	4. Von-Karman Law of the Wall	104
	5. Von Driest Damping Factor	105
	6. Cebeci-Smith Model	105
	7. Baldwin-Lomax Model	105
	8. Far Wake Model	105
XVIII	SUMMARY	107
REFERENCES		108

LIST OF ILLUSTRATIONS

FIGURE		PAGE
1	Aerodynamic Prediction Methods	9
2	Limits of Aerodynamic Theory	10
3	Discretized Velocity Profile	26
4	Cartesian Coordinates with Interpolation on Boundary	
5	Transformed Body-Oriented Coordinates	
6	β Versus Mach Number	64
7	Zones of Energy Excitation	70
8	Wave Diagram for Square Wave Input	80
9	Wave Diagram for Initial Condition Disturbances (Correct Boundary Conditions)	81
10	Wave Diagram for Initial Condition Disturbances (Incorrect Boundary Conditions)	82
11	Surface for Spike-nosed Body	93
12	Flow Field Mesh for Spike-nosed-Body	93
13	Sketch of Physical and Computational Plane	94
14	Viscous Grid Generated about Highly Cambered Airfoil	95

LIST OF TABLES

TABLE		PAGE
1	Required Number of Boundary Conditions	15
2	Summary of Boundary Conditions	17
3	Diagram of Aerodynamics Prediction Levels	17
4	Table of Errors for Blasius Boundary Layer Calculations	30
5	Individual Properties of Air Components	65

LIST OF SYMBOLS

a	speed of sound
A	area
b	slab thickness
c	propagation velocity
C_f	friction coefficient
C_p	specific heat at constant pressure or pressure coefficient
$d = \frac{\nu \Delta t}{\Delta x^2}$	diffusion number
D	diffusion coefficient or Van Direst damping factor
$e = CvT + \frac{V^2}{2}$	internal energy per unit mass
E, F, G	flux vectors in Navier-Stokes equations
E	total energy
$\underline{F}$	vector force
$G(u)$	shock wave variable
$h = C_p T$	enthalpy
$H = C_p T + \frac{V^2}{2}$	total enthalpy
i, j, k	unit vectors for Cartesian coordinates
$\underline{\underline{I}}$	identity matrix in dyadic form
J	Jacobian
L	characteristic length
Le	Lewis number
m	mass
$\dot{m}_i = \delta_i \overline{V}_i$	diffusion flux
M	mach number
p	pressure

LIST OF SYMBOLS (Cont'd)

$\underline{\underline{P}}'$	stress tensor in dyadic form
Pr	Prandtl number
q, r, s	characteristic variables
$\dot{q}$	heat transfer per unit area
$\dot{Q}$	total heat transfer
r	radius
Re	Reynolds number
t	time
T	Temperature
u, v, w	velocity components in Cartesian system
u	flux vector
$\underline{V}$	velocity vector
$\forall$	volume
W	work
x, y, z	coordinates in Cartesian system
$\alpha = \frac{a^{*2}}{U_1^2}$ $= \frac{2\pi\delta}{\lambda}$	parameter in shock relation or wave number
β	damping factor
$\alpha = \frac{Cp}{Cv}$	specific heat ratio
δ	boundary layer thickness
δ^*	displacement thickness
ε	emissivity or eddy viscosity
$\eta = \eta(x,y)$	transformed coordinates
Θ	momentum thickness

LIST OF SYMBOLS (Cont'd)

$\lambda = -2/3\mu$	second viscosity coeff
μ	viscosity
$\nu = \frac{\mu}{\delta}$	kinematic viscosity
$\xi = \xi(x,y)$	transformed coordinates
$\pi = \frac{1}{\gamma} \ln p$	pressure variable
σ	Stephan-Boltzmann constant
σ	normal stress
$\sigma = \frac{c\Delta t}{\Delta x}$	courant number
τ	shear stress
ϕ	velocity potential
$\underline{\omega} = \nabla \times \underline{V}$	vorticity
ρ	density
∇	gradient vector operator

Subscripts

∞	condition at infinity
t	total value
i	species
i,j	grid identifier in space
n	time step identifier
1,2,3	constants
*	sonic condition
11,12,13,22, 23, 33	stress tensor elements

SECTION I

HISTORICAL BACKGROUND

First, a historical review (Reference 1) of aerodynamic theory shall be accomplished in order to obtain an overall perspective. In 1768 D'Alembert, an experimentalist for the King's Navy, used the potential equation of fluid mechanics and showed that, contrary to experimental evidence, zero force was predicted on an arbitrary body immersed in a moving fluid. He stated, "this theory gives absolutely zero resistance: a singular paradox I leave mathematicians to explain." The "D'Alembert paradox" lasted over a century until 1906 when Joukowski introduced the concept of circulation (artifically representing viscous effects) to produce lift. The Wright Brothers flew three years before the Joukowski discovery and obviously used lift. Prandtl's boundary layer concept was employed by Blasius in 1908 to analytically predict friction drag. Charles Lindbergh first crossed the Atlantic in 1927 and Chuck Yeager flew the Bell X-1 supersonically in 1947 which clearly demonstrates the rapid development of aviation during that period.

However, the first large-scale aerodynamic calculation was Kopal's (Reference 2) solution for supersonic flow over cones in 1947. The 308 computed cases required three years for a five-girl team to accomplish using mechanical adding machines. In 1964 Blottner (Reference 3) developed a stable algorithm to solve generalized boundary layers on an electronic computer. Two years prior to this, John Glenn orbited the earth achieving a major breakthrough in our aviation history. In 1971, MacCormack (Reference 4) published the first significant numerical solution of the compressible Navier-Stokes equations.

By contrasting the flight achievements with theoretical aerodynamic development two major points can be made.

1) With aerodynamic theory dramatically lagging, how were the flight achievements possible? The answer is by means of the wind tunnel. Excellent wind tunnel facilities provided the necessary data for the past advancements in aviation.

2) Since the Navier-Stokes equations have been around since 1827 why are we only now able to solve them? The answer is that the solution of the Navier-Stokes equations required the invention of a large-scale computer. The computer only became "of age" during the past decade. Prior to this time only limited analytic calculus solutions of approximate equations could be obtained. Today, a "brute force" method is used to numerically solve the Navier-Stokes equations (Reference 5). The method of Computational Fluid Dynamics (CFD) is based on the fact that a tool is now available that can perform arithmetic very rapidly.

The CRAY-1 computer (Reference 6) can perform over 100 million additions in one second. Previous aerodynamicists had no such tool and their technology developed along other routes. Today, we discretize partial differential equations into finite difference algebraic relationships where arithmetic can be used. Since the large-scale computer is very good at this, the approach is successful.

We are presently developing methods to exploit the computer capabilities. This new field is called "Computational Aerodynamics."

SECTION II

GOVERNING EQUATIONS IN AERODYNAMICS

Various levels of sophistication can be employed to attack a problem in aerodynamics. The approach one takes depends upon the accuracy required, time and funds available, etc. An attempt has been made to catalog the prediction methods to help standardize the nomenclature. Figure 1 lists the methods and restrictions while Figure 2 graphically shows the limits of the methods.

In this section the governing equations of fluid mechanics (Navier-Stokes equations) will be derived. Prior to this derivation however, some vector analysis (Reference 7) relationships must be reviewed.

1. VECTOR ANALYSIS

The following definitions will be required. Examples in Cartesian coordinates are given.

Vector $$\underline{V} = \underline{i}u + \underline{j}v + \underline{k}w$$

Elemental Area $$d\underline{A} = \underline{i}\,dA_x + \underline{j}\,dA_y + \underline{k}\,dA_z$$

Dot Product $$\underline{V}\cdot d\underline{A} = u\,dA_x + v\,dA_y + w\,dA_z$$

Divergence of Vector $$\nabla\cdot\underline{V} = \frac{\partial u + \partial r + \partial w}{\partial x + \partial y + \partial z}$$

Curl of Vector $$\nabla \times \underline{V} = \begin{vmatrix} \underline{i} & \underline{j} & \underline{k} \\ \frac{\partial}{\partial x} & \frac{\partial}{\partial y} & \frac{\partial}{\partial z} \\ u & v & w \end{vmatrix}$$

Dyadic $$\underline{\underline{P}} = \begin{vmatrix} \sigma_{11} & \tau_{12} & \tau_{13} \\ \tau_{21} & \sigma_{22} & \tau_{23} \\ \tau_{31} & \tau_{32} & \sigma_{33} \end{vmatrix}$$

Dot Product of Dyadic

$$\underline{V}\cdot\underline{\underline{P}} = \underline{i}(u\sigma_{11} + v\tau_{21} + w\tau_{31}) + \underline{j}(u\tau_{12} + v\sigma_{22} + w\tau_{32}) + \underline{k}(u\tau_{13} + v\tau_{23} + w\sigma_{33})$$

Divergence of Dyadic

$$\nabla\cdot\underline{\underline{P}} = \underline{i}\left(\frac{\partial\sigma_{11}}{\partial x} + \frac{\partial\tau_{21}}{\partial y} + \frac{\partial\tau_{31}}{\partial z}\right) + \underline{j}\left(\frac{\partial\tau_{12}}{\partial x} + \frac{\partial\sigma_{22}}{\partial y} + \frac{\partial\tau_{32}}{\partial z}\right) + \underline{k}\left(\frac{\partial\tau_{13}}{\partial x} + \frac{\partial\tau_{23}}{\partial y} + \frac{\partial\sigma_{33}}{\partial z}\right)$$

Substantial Derivative

$$\frac{D\underline{V}}{Dt} = \frac{\partial\underline{V}}{\partial t} + (\underline{V}\cdot\nabla)\underline{V} = \frac{\partial\underline{V}}{\partial t} + \nabla\frac{V^2}{2} - \underline{V}\times(\nabla\times\underline{V})$$

Green's Theorem

$$\oint\!\!\!\oint \underline{V}\cdot d\underline{A} = \iiint (\nabla\cdot\underline{V})\, d\forall$$

2. DERIVATION OF NAVIER-STOKES EQUATIONS

The governing equations of fluid mechanics (References 8 and 9) are derived from statements of the conservation of mass, momentum and energy for an arbitrary control volume.

3. CONTINUITY

Statement of the Conservation of Mass

Net Outflow of Mass Through Surface = Decrease of Mass in Control Volume

$$\oiint \rho \underline{V} \cdot d\underline{A} = \frac{\partial m}{\partial t} = -\frac{\partial}{\partial t} \iiint \rho \, d\forall$$

But Green's Theorem states

$$\oiint \rho \underline{V} \cdot d\underline{A} = \iiint (\nabla \cdot \rho V) \, d\forall$$

Hence, after substitution

$$\iiint \left[\frac{\partial \rho}{\partial t} + \nabla \cdot \rho \underline{V} \right] d\forall = 0$$

Since the control volume ($\forall$) is completely arbitrary, the integrand of the integral must vanish.

$$\frac{\partial \rho}{\partial t} + \nabla \cdot \rho \underline{V} = 0 \qquad \text{Continuity Equation}$$

4. MOMENTUM EQUATION

Statement of the Conservation of Momentum

Sum of External Forces = Rate of Change of Momentum

$$\underline{F} = \iiint \rho \frac{D\underline{V}}{Dt} d\forall$$

$$\underline{F} = \text{sum of stresses x Area in unit vector directions}$$

$$= \oiint \underline{\underline{P}} \cdot d\underline{A}$$

Where $\underline{\underline{P}}$ = stress dyadic or stress tensor or stress matrix

A dyadic is treated as a "double vector" and is manipulated as such. It is symmetric and composed of three normal stresses and six shear stresses.

$$\underline{\underline{P}} = (-p + \lambda \nabla \cdot \underline{V})\underline{\underline{I}} + \mu(\nabla \underline{V} + \underline{V}\nabla)$$

Green's theorem is now used as follows:

$$\underline{F} = \oint\!\!\!\oint \underline{\underline{P}} \cdot d\underline{A} = \iiint (\nabla \cdot \underline{\underline{P}})\, d\forall$$

Hence,

$$\iiint \left[\rho \frac{D\underline{V}}{Dt} - \nabla \cdot \underline{\underline{P}}\right] d\forall = 0$$

Similarly, the integrand must vanish. Momentum Equation

$$\rho \frac{D\underline{V}}{Dt} = \nabla \cdot \underline{\underline{P}}$$

5. ENERGY EQUATION

Statement of the Conservation of Energy

Rate of Heat Added	+	Rate of Work Done	=	Rate of Change in Internal Energy

$$\frac{dQ}{dt} + \frac{dW}{dt} = \frac{dE}{dt}$$

$$\oint\!\!\!\oint \underline{\dot{q}} \cdot d\underline{A} + \underline{F} \cdot \underline{V} = \iiint \rho \frac{De}{Dt}\, d\forall$$

$$\oint\!\!\!\oint \left[\underline{\dot{q}} + \underline{\underline{P}} \cdot \underline{V}\right] \cdot d\underline{A} + \quad = \iiint \rho \frac{De}{Dt}\, d\forall$$

where $e = CvT + \frac{V^2}{2}$ and $\underline{\dot{q}} = k\nabla T$

Green's Theorem

$$\iiint \nabla \cdot \left[\underline{\underline{P}} \cdot \underline{V} + \underline{\dot{q}}\right] d\forall = \iiint \rho \frac{De}{Dt}\, d\forall$$

Similarly, the integrand must vanish.

$$\rho \frac{De}{Dt} = \nabla \cdot \left[\underline{\underline{P}} \cdot \underline{V} + \dot{\underline{q}} \right]$$

6. DIVERGENCE FORM OF EQUATIONS

Add the product of 'e' times continuity to the energy equation

$$e \left(\frac{\partial \rho}{\partial t} + \nabla \cdot \rho \underline{V} \right) + \rho \frac{De}{Dt} = e \frac{\partial \rho}{\partial t} + \rho \frac{\rho e}{\partial t} + e \nabla \cdot \rho \underline{V} + \rho \underline{V} \cdot \nabla e$$

$$= \frac{\partial \rho e}{\partial t} + \nabla \cdot \rho \underline{V} e = \nabla \cdot \left[\underline{\underline{P}} \cdot \underline{V} + \dot{\underline{q}} \right]$$

or

$$\frac{\partial}{\partial t}(\rho e) + \nabla \cdot \left[\rho \underline{V} e - \underline{\underline{P}} \cdot \underline{V} - \dot{\underline{q}} \right] = 0$$

Similarly, adding the product of $\underline{V}$ times continuity to the momentum equation produces the divergence form of the momentum equation.

$$\frac{\partial}{\partial t}(\rho \underline{V}) + \nabla \cdot \left[\rho \underline{V} \underline{V} - \underline{\underline{P}} \right] = 0$$

Note that the conservation of mass, momentum and energy can now be written in identical form using the divergence vector in Cartesian coordinates (References 10 and 11).

$$\frac{\partial U}{\partial t} + \frac{\partial E}{\partial x} + \frac{\partial F}{\partial y} + \frac{\partial G}{\partial z} = 0$$

where

$$U = \begin{vmatrix} \rho \\ \rho u \\ \rho v \\ \rho w \\ \rho e \end{vmatrix} \quad i \quad E = \begin{vmatrix} \rho u \\ \rho u^2 - \sigma_{11} \\ \rho uv - \sigma_{12} \\ \rho uw - \tau_{13} \\ \rho ue - u\sigma_{11} - v\tau_{12} - w\tau_{13} - kTx \end{vmatrix}, \text{etc.}$$

where $\rho_{11} = -p + \lambda \nabla \cdot \underline{V} + 2\mu u_x$; $\tau_{12} = \mu(u_y + v_x)$; $\tau_{13} = \mu(u_z + w_x)$

$$\lambda = -\frac{2}{3}\mu$$

The three equations, (2 scalar, 1 vector), contain four unknowns, i.e. ($\underline{V}$, ρ, p, T). The equation of state is needed to close the system. For the present case, an ideal gas is assumed.

$p = \rho R T$; equation of state.

This is the fourth required relationship. Values for the transport and thermodynamic properties (μ, k, Cv, R) are also required as input. These equations with appropriate boundary conditions are capable of representing nearly any aerodynamic problem in the aviation field.

LEVEL	TYPE	LIMITATION	COMPLEXITY	COMPUTER TIME
0	EMPIRICAL	QUALITATIVE	ALGEBRAIC	SEC
I	LINEAR	SMALL α M≠1	↓	↓
II	INVISCID	NO SEPARATION	↓	↓
III	NAVIER–STOKES	NO RESTRICTION	PARTIAL DIFF EQN	HOURS

Figure 1. Aerodynamic Prediction Methods

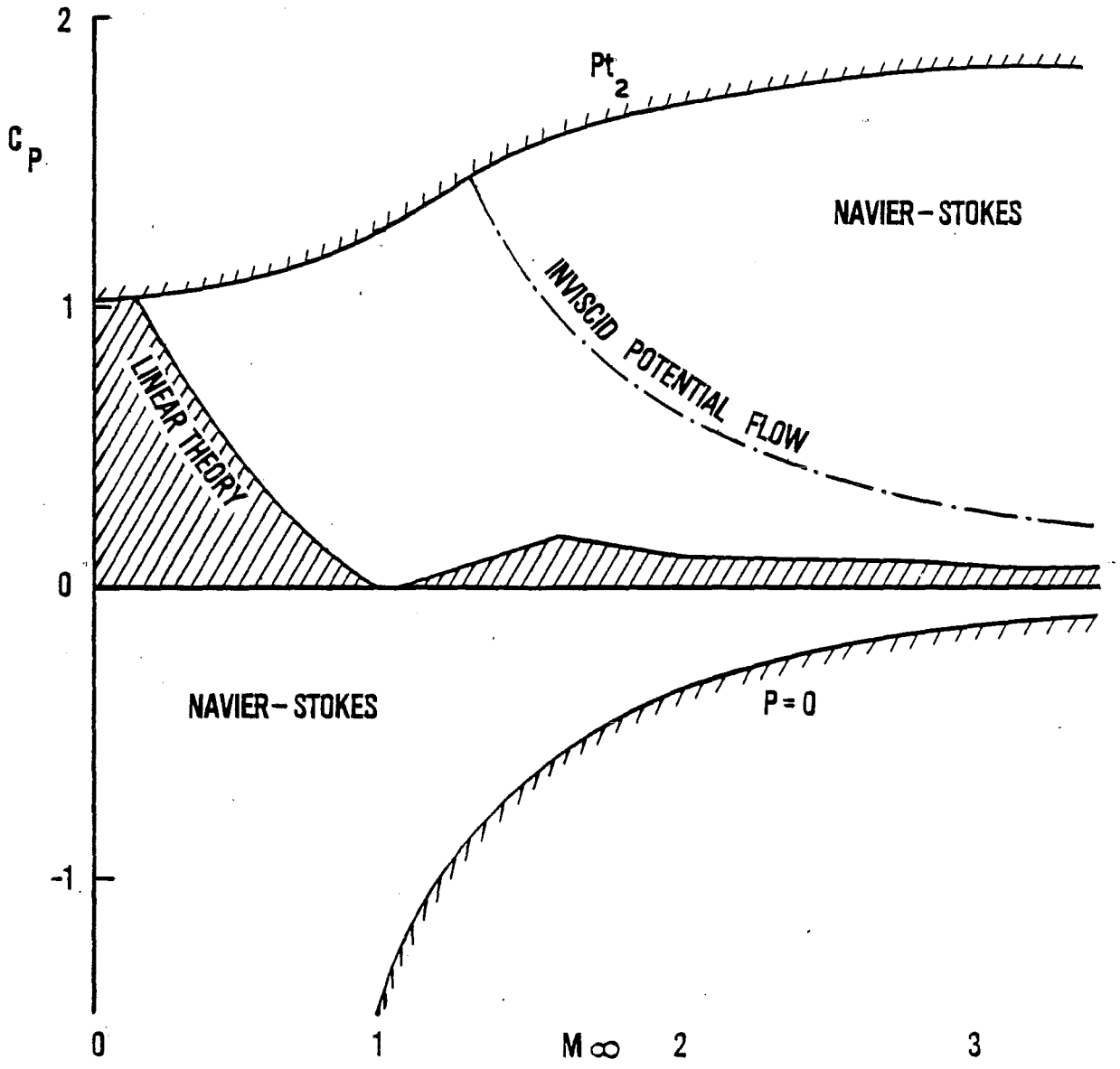

Figure 2. Limits of Aerodynamic Theory

SECTION III

SURVEY OF AERODYNAMIC PREDICTION METHODS

In this section lower forms or approximations of the Navier-Stokes equations will be derived.

1. Level III. Navier-Stokes (References 12 through 20)

$$\frac{\partial U}{\partial t} + \frac{\partial E}{\partial x} + \frac{\partial F}{\partial y} + \frac{\partial G}{\partial z} = 0$$

a. Level III.A Parabolized Navier-Stokes (References 21 and 22)

$$\frac{\partial U}{\partial t} = 0 \therefore \frac{\partial E}{\partial x} = -\frac{\partial F}{\partial y} - \frac{\partial G}{\partial z}$$

where

$$E = \begin{vmatrix} \rho u \\ \rho u^2 + P \\ \rho uv \\ \rho uw \\ \rho ue \end{vmatrix}$$

Viscous terms only in F and G

b. Level III.B Two-D Boundary Layer (References 3 and 23)

$$\frac{\partial U}{\partial t} = 0 \; ; \; \frac{\partial G}{\partial z} = 0$$

$$\underline{\underline{P}} = \begin{vmatrix} -P & \mu Uy \\ \mu Uy & -P \end{vmatrix}$$

or

$$(\rho u)_x + (\rho v)_y = 0$$

$$(\rho u^2 + P)_x + (\rho uv - \mu u_y)_y = 0$$

$$Py = 0$$

$$(\rho uH)_x + (\rho vH - u\tau - kT_y)_y = 0$$

2. LEVEL II

a. Level II.A. Inviscid (Euler) (Referebce 24)

$$\mu = 0 \; ; \; k = 0$$

$$\underline{\underline{P}} = -p\underline{\underline{I}}$$

$$\frac{\partial \underline{U}}{\partial t} = 0$$

$$\nabla \cdot \rho \underline{V} = 0$$

$$\nabla \cdot (\rho \underline{V}\underline{V} + p\underline{\underline{I}}) = 0$$

$$\nabla \cdot (\rho \underline{V} H) = 0$$

where $H = e + \frac{p}{\rho}$

By combining the last equation with the first, one finds that H = constant. Hence one differential equation reduces to an algebraic equation thereby reducing the computer time to solve the system.

Alternate forms of the momentum and energy equations are often used.

$$\frac{D\underline{V}}{Dt} = -\frac{\nabla p}{s} = \frac{\partial \underline{V}}{\partial t} + \nabla \frac{V^2}{2} - \underline{V} \times \underline{\omega} \text{ and } \frac{\rho p}{s} = a^2 = a_o^2 - \frac{\rho - 1}{2} V^2$$

b. Level II.B. Inviscid, Irrotational (Full Potential) (Reference 8)

One of the greatest simplification arises when the vorticity in the flow field is zero, $\underline{\omega} = 0$. This implies that the viscosity vanishes (which was already assumed) and no shocks exist. In practice this means that $M_n < 1.5$ (for which a 7% total pressure drop occurs), and $\frac{P_2}{P_1}(M_n = 1.5) < 2.46$ or only weak shocks are permitted. When this occurs a velocity potential can be introduced.

$$\underline{V} = \nabla\phi$$

Automatically this insures that the vorticity vanish.

$$\underline{\omega} = \nabla \times \underline{V} = \nabla \times \nabla\phi = 0$$

since the Curl of the Gradient vanishes identically. The governing equations becomes as follows:

$$\nabla \cdot \rho \nabla\phi = 0$$

$$\frac{\gamma}{2}\rho\nabla(\nabla\phi)^2 + \nabla(\rho a^2) = 0$$

$$\text{and } a^2 = a_0^2 - \frac{\gamma-1}{2}(\nabla\phi)^2$$

By eliminating ρ these equations produce the full potential equation.

$$a^2\nabla^2\phi = \nabla\phi \cdot (\nabla\phi \cdot \nabla\nabla\phi)$$

Expanding this equation in Cartesian coordinates

$$a^2(\phi_{xx} + \phi_{yy} + \phi_{zz}) = U^2\phi_{xx} + V^2\phi_{yy} + W^2\phi_{zz} + 2UV\,\phi_{xy} + 2UW\phi_{xz} + 2VW\phi_{yz}$$

where $U = \phi_x$

$V = \phi_y$

$W = \phi_z$

3. LEVEL I. LINEARIZED EQUATION (REFERENCES 8 AND 25)

Level I is further restricted by simplifying the non-linear partial differential potential equation to make it linear for which analytic methods of solution have been developed.

Assume small perturbations (Reference 8)

$$U = U_\infty + U'(x,y,z)$$

$$V = V'(x,y,z)$$

$$W = W'(x,y,z)$$

$$\text{or } \phi = XU_\infty + \phi'$$

$$\text{Hence } (1-M_\infty^2)\,\phi'_{xx} + \phi'_{yy} + \phi'_{zz} = 0$$

TABLE 1. REQUIRED NUMBER OF BOUNDARY CONDITIONS

Level III. Navier-Stokes

Variables	Initial Cond. t	B.C. x	B.C. y	B.C. z
u	1	2	2	2
v	1	2	2	2
w	1	2	2	2
P	1	1	1	1
T	1	2	2	2

TOTAL 27 + 5 = 32

Level III.A. Parabolized Navier-Stokes

Variables	Initial Cond. x	B.C. y	B.C. z
u	1	2	2
v	1	2	2
w	1	2	2
P	1	1	1
T	1	2	2

TOTAL 18 + 5 = 23

LEVEL III.B. Two-Dimensional Boundary Layer

Variables	x	y
u	1	2
v	0	1
P	1	1
T	1	2

TOTAL 6 + 3 = 9

TABLE 1. REQUIRED NUMBER OF BOUNDARY CONDITIONS (Continued)

Level II.A. Inviscid (Euler)

Variables	x	y	z
u	1	1	1
v	1	1	1
w	1	1	1
P	1	1	1

TOTAL = 12

Level II.B. Inviscid, Irrotational (Full Potential)

Variables	x	y	z
ϕ	2	2	2

TOTAL = 6

Level I. Linearized Equation

Variables	x	y	z
ϕ	2	2	2

TOTAL = 6

TABLE 2. SUMMARY OF BOUNDARY CONDITIONS

Level	Title	No. Terms	No. B.C.	Restriction
III	Navier-Stokes	77	30	None
	A. Par. N.S.			$\frac{\partial^2}{\partial x^2} = 0$
	B. Boundary Layer			$\frac{v}{u} << 1$
II	Inviscid			
	A. Euler	15	12	$\mu = 0$
	B. Potential	9	6	weak shocks
I	Linear	3	6	$u = v_\infty + u'$

TABLE 3. DIAGRAM OF AERODYNAMIC PREDICTION LEVELS

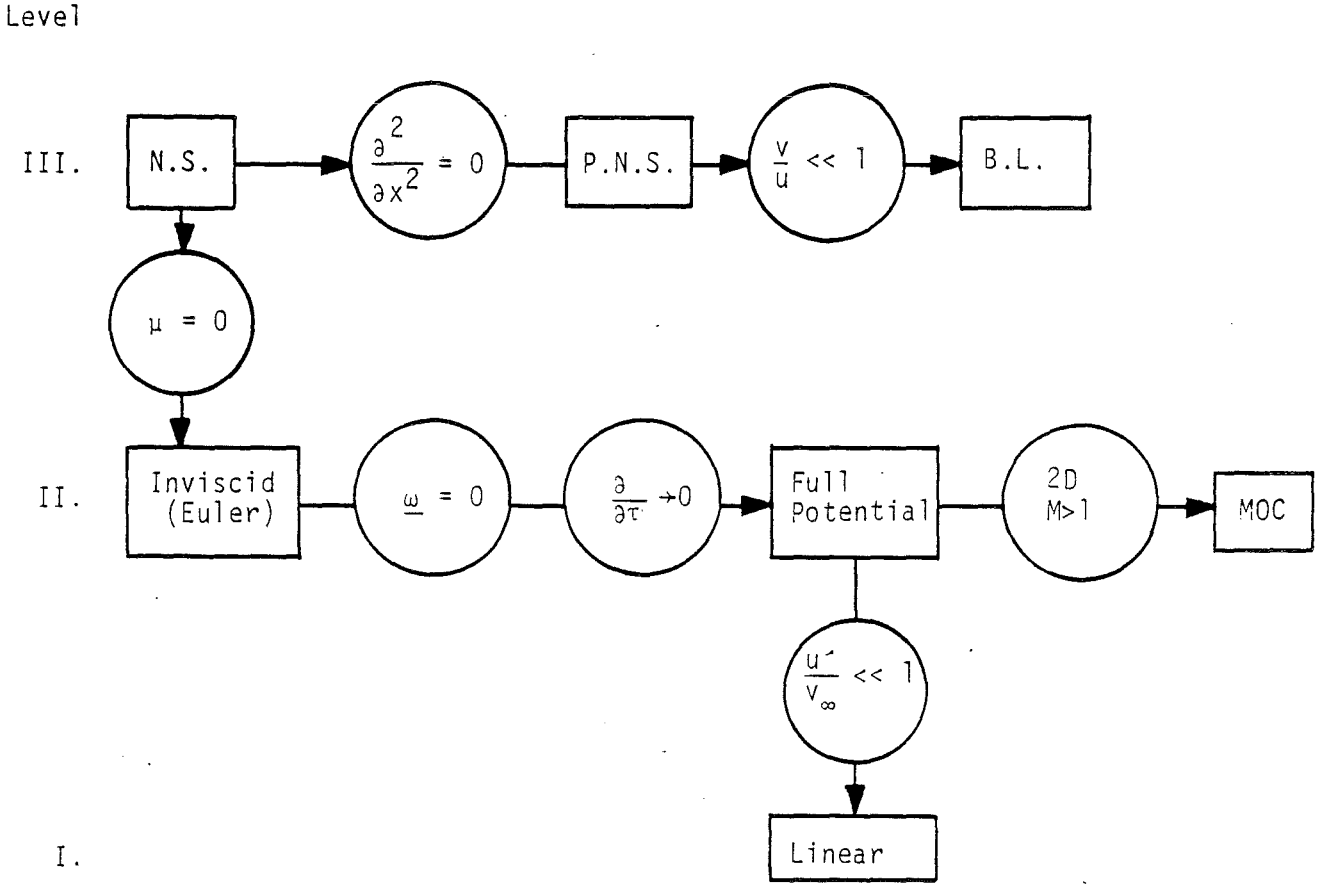

SECTION IV

ANALYTIC SOLUTION OF BOUNDARY LAYERS

One of the first branches of fluid mechanics to exploit numerical methods was the boundary layer field. Most of the important features of CFD can be demonstrated by examining boundary layer solution techniques.

Consider a steady, incompressible, 2-D boundary layer flow (Reference 26).

$$u_x + v_y = 0$$

$$uu_x + vu_y = ue_x + \nu U_{yy}$$

with boundary conditions

$$u(x,0) = 0$$
$$v(x,0) = 0 \qquad u(0,y) = U_\infty$$
$$u(x,\infty) = e\,u(x)$$

For simplicity, consider Blasius flow in which Ue = U_∞.

A transformation is used to realign the coordinates to obtain better numerical accuracy and to simplify the boundary conditions (Reference 27).

Let

$$\xi = x$$

$$\eta = \sqrt{\frac{U_\infty}{2\nu x}}\, y$$

$$F = \frac{U}{U_\infty}$$

$$V = 2\xi\left[\eta_y \frac{v}{U_\infty} + \eta_x F\right]$$

Using the chain rule

$$\frac{\partial}{\partial x} = \xi_x \frac{\partial}{\partial \xi} + \eta_x \frac{\partial}{\partial \eta} = \frac{\partial}{\partial \xi} + \eta_x \frac{\partial}{\partial \eta}$$

$$\frac{\partial}{\partial y} = \xi_y \frac{\partial}{\partial \xi} + \eta_y \frac{\partial}{\partial \eta} = \eta_y \frac{\partial}{\partial \eta}$$

The transformed equations become as follows:

$$V_\eta + F = -2\xi F_\xi$$

$$F_{\eta\eta} - VF_\eta = -2\xi FF_\xi$$

The right-hand sides of these equations are zero for the situation where $F = F(n)$. This type of flow is called "similar" in that all velocity profiles at different stations can be collapsed onto one similar curve. The governing equation then becomes an ordinary differential equation which was first solved by Blasius (1908) using an infinite series (Reference 26).

Let $V = -f$. Hence the governing equation for Blasius flow becomes:

$$f''' + ff'' = 0$$

with boundary conditions

$$f(0) = 0$$

$$f'(0) = 0$$

$$f'(\infty) = 1$$

A series solution is obtained as follows:

Assume $f =$ $$a_0 + a_1\eta + a_2\frac{\eta^2}{2!} + a_3\frac{\eta^3}{3!} + a_4\frac{\eta^4}{4!} + \cdots$$

The solution obtained by substitution of this series into the governing equation and applying inner boundary condition is:

$$f = \frac{a_2\eta^2}{2!} - \frac{a_2^2\eta^5}{5!} + \frac{a_2^3 11\eta^8}{8!}$$

And

$$f''(0)=0.46960=a_2$$

is obtained from the outer boundary condition.

The friction coefficient at the wall is

$$C_f=\frac{\tau_w}{\frac{1}{2}\rho U_\infty^2}=\frac{2\mu}{\rho U_\infty^2}\left(\frac{\partial u}{\partial y}\right)_0=\frac{2\nu\eta_y}{U_\infty}F_\eta(0)=\frac{f''(0)}{\sqrt{\frac{1}{2}Re}}$$

$$\text{or } C_f=\frac{0.66411}{\sqrt{Re}}$$

SECTION V

NUMERICAL SOLUTION OF BOUNDARY LAYERS

With the advent of the digital computer, numerical techniques (Reference 3) were developed because they removed all the limitations required to obtain analytic solutions.

The same transformed boundary layer equations and boundary conditions are used for either the analytic or numerical approach.

$$V_\eta = -F \; ; \quad V(0)=0$$
$$F_{\eta\eta} - V F_\eta = 0 \; ; \quad F(0)=0 \text{ and } F(\infty)=1$$

The velocity profile is discretized into a series of points at equal intervals in η, i.e. $\Delta\eta$ = constant (Figure 3). By using Taylor series, relationships between neighboring points can be obtained (References 28, 29 and 30).

$$F_{n+1} = F_n + F_n' \Delta\eta + F_n'' \frac{\Delta\eta^2}{2!} + F_n''' \frac{\Delta\eta^3}{3!} + F_n^{IV} \frac{\Delta\eta^4}{4!} + \cdots$$

Similarly

$$F_{n-1} = F_n - F_n' \Delta\eta + F_n'' \frac{\Delta\eta^2}{2!} - F_n''' \frac{\Delta\eta^3}{3!} + F_n^{IV} \frac{\Delta\eta^4}{4!} + \cdots$$

By substracting these two relations, one can obtain F_n'.

$$F_n' = \frac{F_{n+1} - F_{n-1}}{2\Delta\eta} - F''' \frac{\Delta\eta^2}{6} + \cdots$$

By adding the two relations one obtains F_n.

$$F_n'' = \frac{F_{n+1} - 2F_n + F_{n-1}}{\Delta\eta^2} - F^{IV} \frac{\Delta\eta^2}{12} + \cdots$$

If we truncate the original Taylor series after the Δn^2 terms we obtain an algebraic finite difference relationship for both the first and second derivatives. Since the governing boundary layer equations have only second derivatives, this "second order" method is sufficient for our purposes.

Using these finite difference relations the governing equation becomes:

$$-a_n F_{n+1} + b_n F_n - c_n F_{n-1} = 0$$

$$a_n = 1 - V_n \frac{\Delta\eta}{2}$$

$$b_n = 2$$

$$c_n = 1 + V_n \frac{\Delta\eta}{2}$$

where V_n is obtained by numerical integration.

$$V = -\int_0^{\eta} F d\eta$$

Using the trapezoidal rule

$$V_n = -\left[F_1 + 2F_2 + 2F_3 + \ldots 2F_{n-1} + F_n\right] \frac{\Delta\eta}{2}$$

or Simpson's Rule

$$V_n = -\left[F_1 + 4F_2 + 2F_3 + \ldots 2F_{n-2} + 4F_{n-1} + F_n\right] \frac{\Delta\eta}{3}$$

Therefore, at each point in the field the governing equation can be expressed only in terms of information available at adjacent points.

The equations for each point developed a regular pattern.

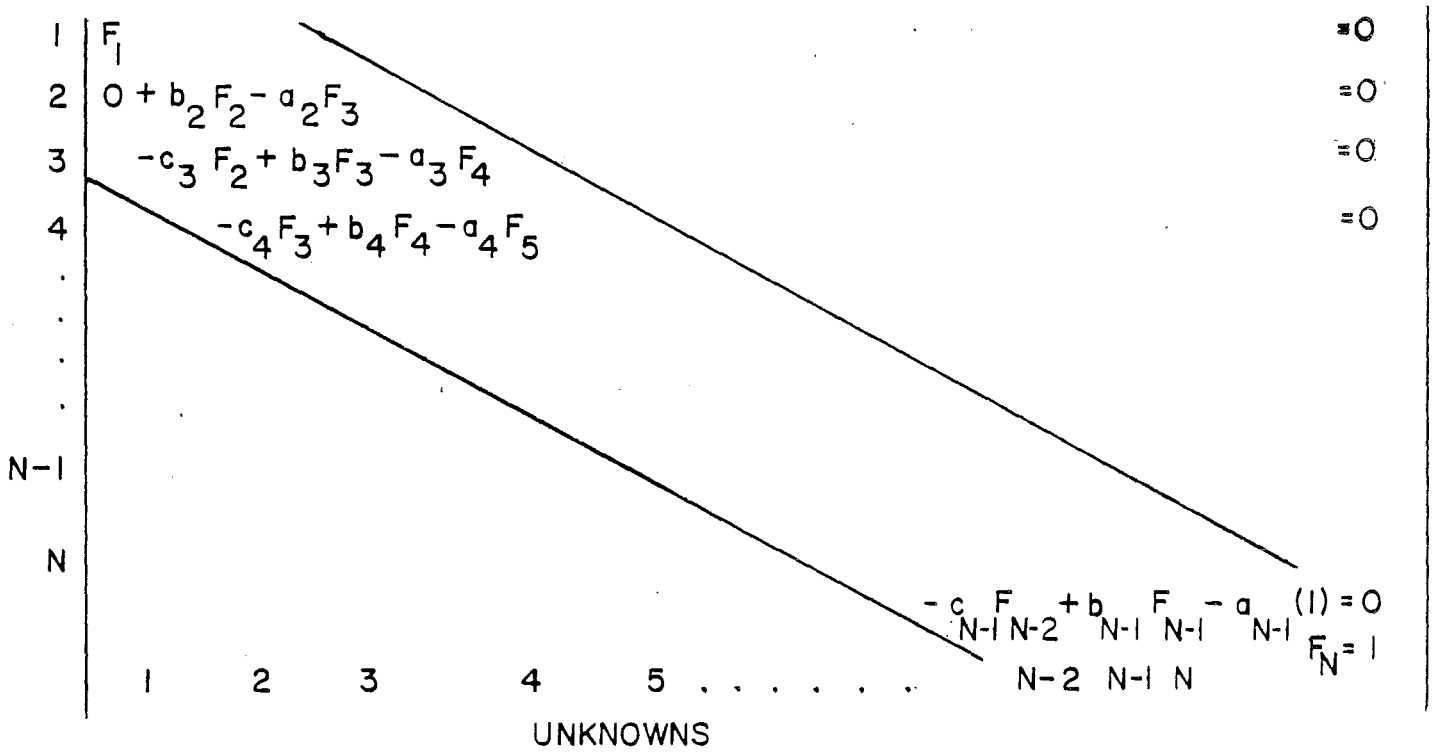

Written in Matrix form, this is called a tri-diagonal matrix.

$$[A]\ |F| = |B|$$

where

$$A = \begin{bmatrix} & & & & o \\ & & & \diagup & \\ & & \diagup & & \\ & \diagup & & & \\ o & & & & \end{bmatrix}$$

We have N linear algebraic equations with constant coefficients (for each iteration cycle) which contain N unknown values of F. To solve this system, we might consider using the standard Cramer's Rule.

$$F_n = \frac{|A-B|}{D}$$

This computation requires (N+1)! multiplications. An estimate of the required computer time can be made for the CRAY-1 which accomplishes 80 million multiplications per second.

N	(N+1)!	CRAY Time
3	24	3×10^{-7} sec
10	39,916,800	0.5 sec
18	1.2×10^{17}	47 years !!!

The surprising escalation of computer time with the number of grid points shows the impracticality of using Cramer's Rule. Fortunately a simple algorithm exists for solving tri-diagonal matrices (which is a form of Gaussian elimination) and is commonly known as the Thomas Algorithm (Reference 3).

Thomas Algorithm

$$-a_n F_{n+1} + b_n F_n - c_n F_{n-1} = d_n \quad \text{where} \quad a_n > 0,\ b_n > 0,\ c_n > 0,\ b_n \geq a_n + c_n$$

Assume the existence of a linear relationship

$$F_n = e_n F_{n+1} + f_n$$

Hence

$$F_{n-1} = e_{n-1} F_n + f_{n-1}$$

Substituting this relationship into the original tri-diagonal and solving for F_n produces the following:

$$F_n = \left(\frac{a_n}{b_n - c_n e_{n-1}}\right) F_{n+1} + \left(\frac{d_n + c_n f_{n-1}}{b_n - c_n e_{n-1}}\right)$$

which confirms the original assumption of a linear relationship, $F_n = e_n F_{n+1} + f_n$.

Therefore

$$e_n = \frac{a_n}{b_n - c_n e_{n-1}}$$

$$f_n = \frac{d_n + c_n f_{n-1}}{b_n - c_n e_{n-1}}$$

The solving procedure is then quite simple. $n > 1$

Starting at the surface where $F_1 = 0$ then $F_1 = e_1 F_2 + f_1 = 0$

We see that $e_1 = 0$ and $f_1 = 0$ (since F_2 is arbitrary in general).

At the next point

$$e_2 = \frac{a_2}{b_2} \qquad f_2 = \frac{d_2}{b_2}$$

and

$$e_3 = \frac{a_3}{b_3 - c_3 e_2}$$

$$f_3 = \frac{d_3 + c_3 f_2}{b_3 - c_3 e_2}$$

etc.

This sweep procedure is continued until e_{N-1} and f_{N-1} are obtained. At this point, we sweep back down and evaluate F_n, using the fact that $F_N = 1$.

$$F_{N-1} = e_{N-1} F_N + f_{N-1} = e_{N-1} + f_{N-1}$$

and using previously evaluated e_n and f_n.

$$F_{N-2} = e_{N-2} F_{N-1} + f_{N-2}$$

.etc.

Continue until all F_n are found.

This procedure is efficient and accurate in that round off errors are seldom encountered. Only three multiplications and two divisions are required at each point. Hence, the computer time is proportional to only kN, which far surpasses the efficiency of Cramer's rule.

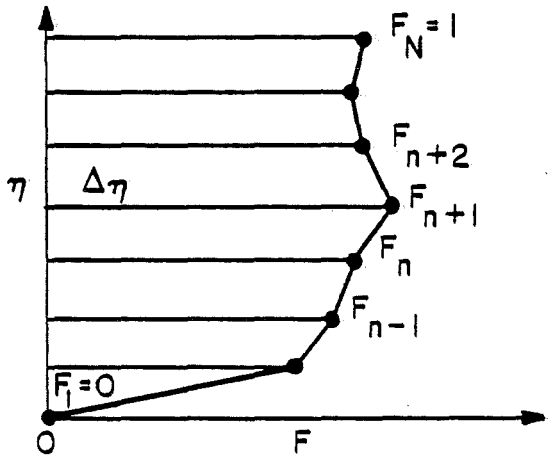

Figure 3. Discretized Velocity Profile

1. SUMMARY OF NUMERICAL PROCEDURE FOR BOUNDARY LAYER CALCULATIONS

By observing the numerical procedure and strategy employed in the solution of boundary layers, we may learn some lessons that will be useful in solving the Navier-Stokes equations. The following are some important steps in the process:

1. Formulate the governing partial differential equations. Insure that

   Number of Unknowns = Number of Equations

   Number of B.C. = Order of Highest Derivative

2. Transform Governing Equations. This simplifies boundary conditions and achieves better numerical accuracy.

3. Convert to Finite Differences

4. Employ Proven Solving Scheme compatible with computer.

5. Satisfy Stability Constraint

6. Keep it Simple Stupid (KISS)

   Maintain lowest order of derivatives in system of equations.

   Avoid elegance and sophistication.

   Make the computer do the work. Minimize your work off the computer. (This is frequently opposite to the strategy in analytic efforts.)

7. Integrate numerically, not analytically. Use graphics to minimize print-out and achieve data compression.

SECTION VI

TRUNCATION ERROR ANALYSIS

Let's return to the formulation of the boundary layer analysis but include higher order terms (References 31, 32, 33 and 34)

$$F''-VF'=-\frac{a_n F_{n-1}+b_n F_n-c_n F_{n+1}-d_n}{\Delta\eta^2}=0$$

where a_n, b_n, c_n retain the same previous definitions but

$$d_n=(F^{IV}-2VF''')\frac{\Delta\eta^4}{12}\equiv\phi\,\frac{\Delta\eta^4}{12}$$

This term is representative of the truncation error in approximating the differential equation by finite differences.

An estimate of the error in wall friction can be obtained by integrating the governing equation.

$$\int_o^\infty F''\,d\eta-\int_o^\infty VF'\,d\eta=\int_o^\infty\left[\frac{-a_nF_{n-1}+b_nF_n-c_nF_{n+1}}{\Delta\eta^2}\right]d\eta-\frac{\Delta\eta^2}{12}\int_o^\infty\phi\,d\eta$$

$$(F')_o^\infty-\left[(VF)_o^\infty-\int_o^\infty V'F\,d\eta\right]=\frac{-\Delta\eta^2}{12}\int_o^\infty\phi\,d\eta$$

since $V'=-F$

$$F'(0)=\int_o^\infty(1-F)F\,d\eta+\frac{\Delta\eta^2}{12}\int_o^\infty\phi\,d\eta=\theta_1+\frac{\Delta\eta^2}{12}\int_o^\infty\phi\,d\eta$$

BUT

$$\int_o^\infty\phi\,d\eta=\int_o^\infty(F^{IV}-2VF''')\,d\eta$$

$$=\left[F'''-2VF''-2FF'\right]_o^\infty+2\int_o^\infty(F')^2\,d\eta$$

$$\int_o^\infty\phi\,d\eta=2\int_o^\infty(F')^2\,d\eta\simeq.7$$

Hence

$$\frac{\Delta F'(0)}{F'(0)} = \frac{\Delta\eta^2}{12(.4696)}(.7) \simeq +.06\,\Delta\eta^2$$

A simple relationship for the error in wall shear stress has been obtained by including the next term in the Taylor series.

1. RICHARDSON'S EXTRAPOLATION

Numerical experiments can be conducted in place of evaluating the function $\int_0^\infty \phi d\eta$ for more complex problems. Recognizing that the truncation error term, for second order methods, will be proportional to $\Delta\eta^2$, a technique can be developed which can extrapolate the results to zero error.

Write two experssions for the error for two different step size calculations

$$F_1' - F'(\text{exact}) = k\,\Delta\eta_1^2$$

$$F_2' - F'(\text{exact}) = k\,\Delta\eta_2^2$$

By dividing these two equations, k (which in general, is difficult to evaluate analytically) can be eliminated. The exact value then can be predicted.

$$F'(\text{exact}) = \frac{F_1' - \left(\frac{\Delta\eta_1}{\Delta\eta_2}\right)^2 F_2'}{1 - \left(\frac{\Delta\eta_1}{\Delta\eta_2}\right)^2}$$

This is known as Richardson's extrapolation and is a practical method for error estimation.

Below is a tabulation for Blasius boundary layer calculations of the error term in wall friction for different $\Delta\eta$ step size.

TABLE 4

TABLE OF ERRORS FOR BLASIUS BOUNDARY LAYER CALCULATIONS

$\Delta\eta$	F'(o)	Error	%	$\frac{\Delta F'(o)12}{F'(o)\ \Delta\eta^2}$	F'(o) Richardson's Extrapolation	Error
0	.46960	0	---	---		
.1	.46966	+ .00006	---	.146	.46959	-.0001
.2	.46988	.00028	---	.179		
.25	.47004	.00044	.09%	.180	.46947	-.00001
.5	.47140	.00180	.38	.184	.46959	-.00013
1.0	.47718	.00758	1.6	.194	.46957	-.00001
2.0	.50	.0304	6.5	.194	.330476	-.1391
5.0	1.39	.92	200	.94		

SECTION VII

STABILITY ANALYSIS

The major issue in choosing a finite difference algorithm is its stability characteristics. Of the many, many ways to represent a partial differential equation by finite differences only a few are stable. (Many come forth but few are chosen). The best way to appreciate this is to consider the roots of a very high degree polynomial of order n. To insist that no positive real root exists when n equals several thousand is a severe restriction. This is equivalent to demanding that no positive real eigenvalues be permitted in the large solution matrix representing the entire computational grid.

Since many points exist then this is obviously a very severe constraint. Therefore, most of us should use only proven algorithms and not invent new ones.

1. MODEL EQUATIONS

To study stability, we shall use linear model equations to demonstrate the key features (Reference 35, 36 and 37).

The boundary layer equation has terms that represent advection (convection) and diffusion of the following form:

$$U_t + UU_x + VU_y = \nu U_{yy}$$

These two processes can be represented by two simple model equations.

Advection $U_t + cU_x = 0$	Simple wave equation.
Diffusion: $U_t = \nu U_{xx}$	Heat equation.

By examining the stability of these two equations, the major limitations can be assessed. This greatly reduces the amount of labor involved.

2. VON NEUMANN STABILITY ANALYSIS

Let us first consider two possible finite difference representation of the simple wave equation (Reference 31).

1. Forward Time - Central Space (FTCS) Differencing Scheme

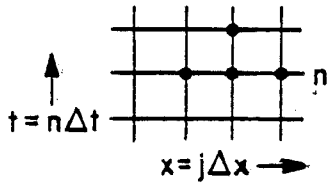

$$U_t + cU_x = \frac{U_j^{n+1} - U_j^n}{\Delta t} + \frac{c(U_{j+1}^n - U_{j-1}^n)}{2\Delta x} = 0$$

2. Backward Time - Central Space (BTCS)

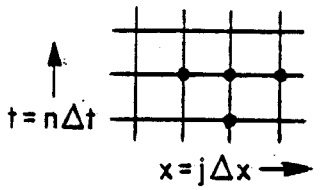

$$U_t + cU_x = \frac{U_j^{n+1} - U_j^n}{\Delta t} + c\,\frac{U_{j+1}^{n+1} - U_{j-1}^{n+1}}{2\Delta x}$$

Defining $\sigma = \frac{c\Delta t}{\Delta x}$ = Courant Number

Hence

FTCS:
$$U_j^{n+1} = -\frac{\sigma}{2} U_{j+1}^n + U_j^n + \frac{\sigma}{2} U_{j-1}^n$$

BTCS:
$$U_j^n = \frac{\sigma}{2} U_{j+1}^{n+1} + U_j^{n+1} - \frac{\sigma}{2} U_{j-1}^{n+1}$$

Von Neumann (1944) devised a method for analyzing the stability of finite difference relationships. A Fourier series expansion of the solution is performed and the decay or amplification of each mode is examined to determine the stability characteristics.

Let

$$U^n = \hat{U}^n(t) e^{i\alpha x}$$

where $\hat{U}^n(t)$ is the amplitude function at time-level n and α is the wave number. $(i=\sqrt{-1})$

Hence: FTCS: $$\hat{U}^{n+1} e^{i\alpha x} = \hat{U}^n \left[-\frac{\sigma}{2} e^{i\alpha(x+\Delta x)} + e^{i\alpha x} + \frac{\sigma}{2} e^{i\alpha(x-\Delta x)} \right]$$

and Gain $$= G = \frac{\hat{U}^{n+1}}{\hat{U}^n} = 1 + \frac{\sigma}{2}\left(e^{-i\alpha\Delta x} - e^{i\alpha\Delta x}\right)$$

or $$G = 1 - i\sigma \sin(\alpha\Delta x) = \text{AMPLIFICATION FACTOR}$$

For stability, $|G| < 1$, since the solution must remain bounded.

$$G\bar{G} = 1 + \sigma^2 \sin^2 \alpha\Delta x < 1$$

The stability criteria indicates that $\sigma = 0$ is required, which is impossible to achieve.

Therefore FTCS = unconditionally unstable.

Likewise,

BTCS $$\hat{U}^n = \hat{U}^{n+1}\left[1 + \frac{\sigma}{2}\left(e^{i\alpha\Delta x} - e^{-i\alpha\Delta x}\right)\right]$$

or $$G = \frac{\hat{U}^{n+1}}{\hat{U}^n} = \left[1 + i\sigma \sin\alpha\Delta x\right]^{-1}$$

$$G\bar{G} = \frac{1}{1 + \sigma^2 \sin^2 \alpha\Delta x} < 1$$

$$|G| = \frac{1}{\sqrt{1+\sigma^2 \sin^2 a\Delta x}} < 1$$

For stability σ = any value. Therefore BTCS is unconditionally stable.

3. SUMMARY Simple wave equation

FTCS: any σ or any step size is unstable.

BTCS: any σ or any step size is stable.

4. EIGENVALUE INTERPRETATION OF GAIN

Let $\hat{U}^n = Ae^{\lambda t}$

Hence $\hat{U}^{n+1} = Ae^{\lambda(t+\Delta t)}$

Therefore $G = \frac{\hat{U}^{n+1}}{\hat{U}^n} = e^{\lambda \Delta t} = 1 + \lambda \Delta t \ldots$

$G < 1$ means $\lambda \Delta t < 0$

Since $\Delta t > 0$ this means

$\lambda < 0$ or no positive, real eigenvalue in time is permitted.

5. DIFFUSION EQUATION

Similarly for the Diffusion Equation

$$U_t = \nu U_{xx} \quad \text{Let } d = \frac{\nu \Delta t}{\Delta x^2} = \text{Diffusion Number}$$

FTCS

$$\frac{U_j^{n+1} - U_j^n}{\Delta t} = \frac{\nu(U_{j+1}^n - 2U_j^n + U_{j-1}^n)}{\Delta x^2}$$

Hence the Von Newmann Stability analysis produces

$$G = 1 - 2d\,(1 - \cos\alpha\Delta x)$$

Since

Since $|G| < 1$

$|2d|(1-\cos\alpha\Delta x) - 1| < 1$; But $(1-\cos\alpha\Delta x) = 2$ Maxvalue

Therefore $d < \frac{1}{2}$ · Conditionally Stable.

Likewise

BTCS:

$$G = \left[1 + 2d\,(1 - \cos\alpha\Delta x)\right]^{-1}$$

$|G| < 1$ $\nu > 0$

$\Delta t > 0$ Always true

$\Delta x^2 > 0$

$d > 0$ Unconditionally Stable

SECTION VIII

NUMERICAL ALGORITHMS

In this section some of the classical differencing schemes will be examined. A few will be selected which are representative of the methods in use today. Hopefully, an understanding will be developed from studying these few cases which will enable the reader to interpret other methods with ease.

The cases to be investigated are (Reference 31):

1. Leapfrog Explicit
2. MacCormack Explicit
3. Fully Implicit
4. Crank-Nicholson Implicit

Roache (CFD) lists several other methods which should be reviewed.

1. EXPLICIT METHODS

An explicit method is one in which all of the values on the right-hand side of the difference equation needed to calculate the advance time level values of U^{n+1} are known. Methods wherein U^{n+1} also appears on the right-hand side are called implicit and generally require a matrix inversion to calculate a new time level.

2. MIDPOINT LEAPFROG METHOD

The leapfrog method is a single step, second order accurate explicit method (Reference 36). Since the method is central in time, three time levels are involved. The term "leapfrog" is derived from the fact that the new values are calculated at each other time level, skipping the time level in between.

Consider the wave equation:

$$\frac{\partial u}{\partial t} + c\frac{\partial u}{\partial x} = 0$$

$$\frac{U_i^{n+1} - U_i^{n-1}}{2\Delta t} + c\frac{U_{i+1}^{n} - U_{i-1}^{n}}{2\Delta t} = 0$$

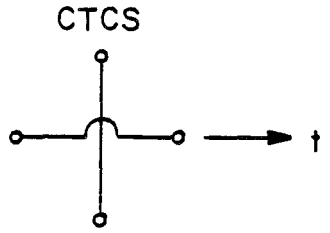

Recombining

$$U_i^{n+1} = U_i^{n-1} - \sigma(U_{i+1}^{n} - U_{i-1}^{n})$$

where $\sigma = c\frac{\Delta t}{\Delta x}$ Courant number (Ref 38)

The stability may be assessed using the Von Neumann method.

Let $U^n = \hat{U}^n(t)\, e^{i\alpha x}$, then

$$\hat{U}^{n+1} = \hat{U}^{n-1} - \sigma\hat{U}^n(e^{i\alpha\Delta x} - e^{-i\alpha\Delta x})$$

$$\text{or}\ \hat{U}^{n+1} = \hat{U}^{n-1} - i(2\sigma\sin\alpha\Delta x)\hat{U}^n \equiv a\hat{U}^n + \hat{U}^{n-1}$$

Since this is a multi-time level method, an identity relation must be added to determine the amplification factor, i.e.

$$\hat{U}^n = (1)\hat{U}^n + 0(\hat{U}^{n-1})$$

Hence

$$\begin{vmatrix} \hat{U}^{n+1} \\ \hat{U}^{n} \end{vmatrix} = G \begin{vmatrix} \hat{U}^{n} \\ \hat{U}^{n-1} \end{vmatrix} \quad \text{where } G = \begin{vmatrix} a & 1 \\ 1 & 0 \end{vmatrix}$$

For the previous one-level method, G was simply a number, and the stability criterion was $|G| \leq 1$.

For the present case where G is a matrix $\underline{\underline{G}} - \lambda\underline{\underline{I}} = 0$

then, $\lambda < 1$ is the stability criterion. Another frequently used statement is that the "spectral radius" of G must be less than unity.

$$\underline{\underline{G}} - \lambda \underline{\underline{I}} = \begin{vmatrix} a-\lambda & 1 \\ 1 & (0-\lambda) \end{vmatrix} = 0$$

$$\text{or } \lambda^2 - a\lambda - 1 = 0$$

Hence

$$\lambda = \frac{1}{2}(a \pm \sqrt{a^2+4})$$

Inserting a into the equation, Roache shows that $\lambda = 1$ for $\sigma \leq 1$. This indicates that the leapfrog scheme is marginally-conditionally stable.

3. MACCORMACK EXPLICIT METHOD (REFERENCE 4)

An extremely popular method for solving compressible flows has been the method of MacCormack (1971). It is a two step method which alternately uses forward and backward differences (References 39, 40). Although each step is first order, the result after the two-step cycle is second order accurate in both time and space.

Consider the model equation: $U_t + C\,U_x = 0$

Forward Predictor (FTFS) Step

$$\frac{U_i^{n+\frac{1}{2}} - U_i^n}{\Delta t} + c\,\frac{U_{i-1}^n - U_i^n}{\Delta x} = 0$$

Backward Corrector (FTBS) Step

$$\frac{U_i^{n+1} - U_i^n}{\Delta t} + c\,\frac{U_i^{n+\frac{1}{2}} - U_{i-1}^{n+\frac{1}{2}}}{\Delta x} + c\,\frac{U_{i+1}^n - U_i^n}{2\Delta x} = 0$$

$$\text{or } U_i^{n+1} = \frac{1}{2}\left[U_i^n + U_i^{n+\frac{1}{2}} - \sigma\,(U_i^{n+\frac{1}{2}} - U_{i-1}^{n+\frac{1}{2}})\right]$$

$$\text{where } U_i^{n+\frac{1}{2}} = U_i^n(1+\sigma) - \sigma\,U_{i+1}^n$$

Performing a stability analysis

$$2\hat{U}^{n+1} = \hat{U}^{n} + \hat{U}^{n+\frac{1}{2}}\left[(1-\sigma) + \sigma e^{-i\alpha\Delta x}\right]$$

$$\text{and } \hat{U}^{n+\frac{1}{2}} = \hat{U}^{n}\left(1+\sigma-\sigma e^{i\alpha\Delta x}\right)$$

eliminating $\hat{U}^{n+\frac{1}{2}}$

$$G = \frac{\hat{U}^{n+1}}{\hat{U}^{n}} = \frac{1}{2} + \frac{1}{2}\left(1-\sigma+\sigma e^{-i\alpha\Delta x}\right)\left(1+\sigma-\sigma e^{i\alpha\Delta x}\right)$$

$$\text{or } G = 1-\sigma^{2}(1-\cos\alpha\Delta x) - i\sigma\sin\alpha x$$

Stability Condition

$$G\bar{G} = 1-(1-\cos\alpha\Delta x)^{2}\sigma^{2}(1-\sigma^{2}) < 1$$

This condition is satisfied provided $\sigma < 1$. Therefore, MacCormack's method is conditionally stable.

4. FULLY IMPLICIT (REFERENCE 31)

The methods previously described are explicit, in that only known values at previous time levels are needed to advance the calculation to the new time level $^{(n+1)}$. We will now discuss implicit methods, which use new values in the spatial derivatives, thereby requiring the simultaneous solution of equations at (n+1) in order to advance the calculations.

Write the model equation

$$U_t + CU_x = 0$$

in finite difference form

using FTCS but evaluating the advection term at the new time level (n+1).

This if the fully implicit method.

$$\frac{U_i^{n+1} - U_i^n}{\Delta t} + c\,\frac{\left(U_{i+1}^{n+1} - U_{i-1}^{n+1}\right)}{2\Delta x} = 0 \qquad \text{Error } (\Delta t, \Delta x^2)$$

$$U_i^{n+1} = U_i^n - \frac{\sigma}{2}\left(U_{i+1}^{n+1} - U_{i-1}^{n+1}\right)$$

Using the Von Neumann stability analysis

$$\hat{U}^{n+1}(1 + i\sigma \sin\alpha\Delta x) = \hat{U}^n$$

$$\text{Hence } G = \frac{1}{1 + i\sigma\sin\alpha\Delta x}$$

$$\text{or } G\bar{G} = \frac{1}{1 + \sigma^2 \sin^2\alpha\Delta x} < 1$$

Since any value of σ will achieve the stability condition, the fully implicit method is unconditionally stable.

5. CRANK NICOLSON IMPLICIT (REFERENCE 41 AND 42)

A modification of the above implicit method is to use FTCS but evaluate the advection term at the average between the (n) and (n+1) terms.

For the model equation this scheme, developed by Crank-Nicholson (1947), is the following

$$\frac{U_i^{n+1} - U_i^n}{\Delta t} + c\,\frac{(U_{i+1}^{n+1} - U_{i-1}^{n+1})}{4\Delta x} + c\,\frac{(U_{i+1}^{n} - U_{i-1}^{n})}{4\Delta x} = 0 \qquad \text{Error} = (\Delta t^2, \Delta x^2)$$

The amplification factor is

$$G = \frac{\hat{U}^{n+1}}{\hat{U}^{n}} = \frac{1 - i\frac{\sigma}{2}\sin\alpha\Delta x}{1 + i\frac{\sigma}{2}\sin\alpha\Delta x}$$

For which $G\bar{G} = 1$ which is marginally stable.

SECTION IX

SHOCK WAVE STRUCTURE

Consider a traveling shock wave in a long tube (Reference 8). In most aerodynamic calculations a shock wave is treated as a discontinuity and Rankine-Hugoniot relations are used. However, a shock wave in nature has a continuous structure which establishes a rapid transition from one state to another. To analyze this situation we shall utilize the unsteady Navier-Stokes equations in one spatial dimension.

$$U_t + E_x = 0$$

$$\text{where } U = \begin{vmatrix} \rho \\ \rho u \\ \rho e \end{vmatrix} \; ; \quad E = \begin{vmatrix} \rho u \\ \rho u^2 - \sigma_{11} \\ \rho u e - u\sigma_{11} - kTx \end{vmatrix}$$

$$\text{and } e = C_v T + \frac{u^2}{2} = H - \frac{P}{\rho}$$

$$\sigma_{11} = -P + \lambda u_x + 2\mu u_x = -P + \frac{4}{3}\mu u_x$$

$$\text{since } \lambda = -\frac{2}{3}\mu \text{ and } \mu = \mu(T)$$

The energy equation can be simplified for the case in which $P_r = \frac{\mu C_p}{K} = 3/4$

In reality Prandtl number for air is 0.72, making this approximation quite reasonable. Using this condition the energy equation becomes

$$\rho u e - u\sigma_{11} - kTx = \rho u\left(e + \frac{P}{\rho}\right) - \frac{4}{3}\mu u u_x - kTx$$

$$= \rho u H - \frac{4}{3}\mu H x - kTx\left(1 - \cancel{\frac{4}{3}}^{\,0} Pr\right)$$

First an analytic solution shall be obtained and then the numerical procedure discussed.

1. ANALYTIC SOLUTION (REFERENCE 43)

First transform to eliminate the variation of $\mu(T)$ effects.

$$\text{Let } d\xi = \frac{3}{4\mu}\, dx$$

$$\text{Hence } \frac{4\mu}{3}\begin{vmatrix}\rho\\ \rho u\\ \rho e\end{vmatrix}_t + \begin{vmatrix}\rho u\\ \rho u^2 + P - u_\xi\\ \rho u\, H - H_\xi\end{vmatrix}_\xi = 0$$

For steady state this equation may be immediately integrated.

$$\rho u = C_1$$

$$\rho u^2 + P - u_\xi = C_1 C_2 = C_1 u + P - u_\xi$$

$$\rho u\, H - H_\xi = C_1 C_3 = C_1 H - H_\xi$$

The last equation can be integrated again.

$$H = C_3 + C_4 e^{C_1 \xi}$$

Since for no heat addition H ($\xi \to \infty$) must be bounded we conclude that $C_4 = 0$, and hence $H = C_3 = \text{constant} = H_1$. We will find it useful to express H_1 in terms of the acoustic speed.

$$H_1 = \frac{\gamma+1}{2(\gamma-1)}\, a_*^2 = H$$

thus

$$\frac{a^2}{\gamma u} = \frac{\gamma P}{\rho} = \frac{\gamma+1}{2}\, a_*^2 - \frac{\gamma-1}{2}\, u^2$$

Therefore p can be eliminated from the momentum equation.

$$\rho u^2 + P = C_1 \left(u + \frac{a^2}{\gamma u}\right) = C_1 C_2 + u_\xi$$

since $a^2 = a^2(u)$ this equation can now be integrated. Inserting a^2 into the momentum equation and regrouping produces the following:

$$(1-\frac{u}{u_1})(\frac{u}{u_1}-\alpha) = -\frac{a^2}{\gamma u}\frac{uu_\xi}{C_1}$$

Note: $C_1 = \rho_1 u_1$

$$C_2 = \frac{\gamma+1}{2\gamma} u_1 (1+\alpha)$$

$$\alpha = \frac{a_*^2}{u_1^2}$$

By Integrating once more the distribution of u through a shock wave is obtained.

$$(1-\frac{u}{u_1})(\frac{u}{u_1}-\alpha)^{-\alpha} = C_5 e^{(1-\alpha)\frac{\gamma+1}{2\gamma}\int^3 \frac{\rho_1 u_1 dx}{4\mu}}$$

The final integration constant C_5 is determined by arbitrarily setting $x = 0$ at some reference point. One possibility is to select $x = 0$ at $u = a^*$ since it must always occur in the interval of the shock.

Hence

$$C_5 = \frac{1-\sqrt{\alpha}}{(\sqrt{\alpha}-\alpha)^\alpha}$$

Note that the Rankine-Hugoniot condition is recovered in the asymptotic limit.

$$x \to -\infty; \left(\frac{u}{u_1}\right)_1 = 1$$

$$x \to +\infty \left(\frac{U}{U_1}\right)_2 = \alpha = \frac{a^{*2}}{u_1^2}$$

$$\text{or } u_1 u_2 = a^{*2}$$

(Prandtl's Relation Reference 44)

2. SUMMARY OF FIVE BOUNDARY CONDITIONS

	Given
$C_1 = \rho_1 u_1$	; $\rho_1 u_1$
$C_2 = \frac{\rho_1 u_1^2 + P_1}{\rho_1 u_1} = (1+\alpha)\frac{\gamma+1}{2\gamma}$	; u_1
$C_3 = H_1 = \frac{\gamma+1}{2(\gamma-1)} a_*^2$	; H_1
$C_4 = 0$ or $H_2 = H_1$	; $Hx = 0$ at ∞
$C_5 = \frac{1-\sqrt{\alpha}}{(\sqrt{\alpha}-\alpha)^{\alpha}}\alpha$; $u(0) = a^*$	; $u(0) = a^*$

3. Numerical Solutions Returning to the Governing Equation

$$U_t + Ex = 0$$

we wish to conduct a numerical integration.

However in order to reduce the amount of programming we shall make use of some of the analytic results. Let $\rho u = C_1$ and $H = C_3$ and hence only the momentum equation requires numerical integration.

$$(\rho u)_t + (\rho u^2 - \sigma_{11})_x = 0$$

$$u\left[\rho_t + (\rho u)_x\right] + \rho u_t + \rho u u_x - (\sigma_{11})_x = 0$$

Divide by ρ

$$u_t + u u_x + \frac{1}{\rho}\left(\frac{\rho a^2}{\gamma} - \frac{4}{3}\mu u_x\right)_x = 0$$

Rewriting: $u_t + u G_x = 0$

Where
$$G = u + \frac{a^2}{\gamma u} - \frac{4}{3}\frac{\mu}{C_1} u_x \equiv G(u)$$

To solve the above equation for u(x) we shall use MacCormack's two-step difference scheme.

Forward Predictor
$$u_i^{n+\frac{1}{2}} = u_i^n \left[1 - \frac{\Delta t}{\Delta x}\left(G_{i+1}^n - G_i^n\right)\right]$$

Backward Corrector
$$u_i^{n+1} = \frac{1}{2} u_i^n + \frac{1}{2} u_i^{n+\frac{1}{2}} \left[1 - \frac{\Delta t}{\Delta x}\left(G_i^{n+\frac{1}{2}} - G_{i-1}^{n+\frac{1}{2}}\right)\right]$$

Care must be exercised in evaluating the derivatives in G.

BACKARD IN PREDICTOR
$$G_i^n = u_i^n + \left(\frac{a_i^2}{a u_i}\right)^n - \left(\frac{4\mu}{3C_i}\right)\left(\frac{u_i^n - u_{i-1}^n}{\Delta x}\right);$$

FORWARD IN CORRECTOR
$$G_i^{n+\frac{1}{2}} = u_i^{n+\frac{1}{2}} + \left(\frac{a_i^2}{a u_i}\right) - \left(\frac{4\mu}{3C_i}\right)\left(\frac{u_{i+1}^{n+\frac{1}{2}} - u_i^{n+\frac{1}{2}}}{\Delta x}\right);$$

4. FIVE BOUNDARY CONDITIONS

1. $\rho_1 u_1 = C_1$

2 and 3. $H_1 = C_3 = H_2 = \frac{\gamma+1}{2(\gamma-1)} a_*^2$

4. $u_1(-x_1) = u_1$

5. $u(0) =$ a Arbitrary Origin Reference

or $u_2(+x_2) = u_2$

SECTION X

ARTIFICIAL VISCOSITY

Before obtaining a numerical solution one should examine the length scales appearing in the Navier-Stokes equations. To accomplish this we shall examine the dimensionless independent variables. They are of the following form:

$$1.\ \frac{tu_1}{L}$$

$$2.\ \frac{x}{L}$$

$$3.\ \frac{u_1 x}{\nu}$$

We first see a time scale of $\frac{L}{U}$. This term is defined as a characteristic time (t_{ch}) which equals the time required for a particle to traverse the computational domain (L). A characteristic time (t_{ch}) is a good measure of the time for transient phenomenon to occur. Generally the inviscid field requires about 3 t_{ch} to attain steady state based upon both shock tunnel and numerical experience.

In space we have a scale length of L which is derived from the boundary conditions imposed at the edge of the computational domain. The other length scale is $\frac{\nu}{U_1}$ which is proportional to the mean free path.

$$\tilde{\lambda} = 1.62\frac{\nu}{a} = \text{mean free path} \simeq 10^{-6}\ \text{ft at sea level}$$

Since in practical problems these two-scale lengths are orders of magnitude apart it is apparent that numerical difficulties should be anticipated.

A derived intermediate scale arising in solving these problems results from a combination of the previous two scales.

$$\delta = \sqrt{L\tilde{\lambda}} = \frac{L}{\sqrt{\frac{u_1 L}{\nu}}} = \text{Boundary Layer Thickness}$$

In engineering practice we attempt to honor both L and δ but disregard $\tilde{\lambda}$ as being unimportant.

Assume

$$\frac{\Delta x}{L} \ll 1$$

$$\frac{\Delta x}{\delta} < 1$$

$$\frac{\Delta x}{\tilde{\lambda}} \gg 1$$

The equations and numerical solving technique are unaware of our intentions and regard the small scale lengths as introducing mathematical "stiffness" into the problem. Numerical instabilities occur if calculations are attempted with this disparity existing. In computing shock waves, for example, oscillations occur (Gibbs phenomena) since the shock thickness is far less than the step size used in engineering practice. To eliminate this problem an aritifice is required. Since we cannot make $\Delta x < \tilde{\lambda}$ and solve any practical problem, let's multiply $\tilde{\lambda}$ by a factor (β) to make it as large as Δx.

$$\text{Let } \Delta x = \beta\tilde{\lambda}$$

$$\text{Therefore } \beta\tilde{\lambda} = \frac{1.6\beta\mu}{a\rho} = \Delta x$$

Let $\mu' = \beta\mu$ which is <u>artificial viscosity</u> added to the equation to remove the mathematical difficulty (References 45, 46 and 47).

This procedure obviously changes the physics of the problem, however, and we must exercise care that the additional viscosity effects are no greater then the truncation error in the finite difference scheme. If this objective can be obtained we have a practical solution to the numerical difficulty. Several forms of artificial viscosity shall now be discussed.

1. NORMAL STRESS DAMPING (REFERENCE 2)

In the normal stresses two viscosity terms appear,

$$\sigma_{11} = -P + \lambda \nabla \cdot \underline{V} + 2\mu u_x$$

$$\text{where } \lambda = -\frac{2}{3}\mu$$

$$\text{Rewrite this term } \lambda = +\frac{2}{3}\beta\mu$$

$$\text{where } \beta \cong \frac{u_1 \Delta x}{\nu} = \text{Cell Reynold's Number}$$

This scheme has been used successfully by McRae in treating the shock wave for a cone at angle-of-attack

The shear terms, e.g. $\tau_{12} = \mu\ (u_y + v_x)$, are unaltered in this approach. Since λ is only of any consequence in the normal stresses, it improves the shock capturing capability without affecting the shear terms.

2. VON NEUMANN RICHTMYER DAMPING

The first to use artificial viscosity merely added a term to the Euler equation in place of the non-existent Navier-Stokes stress terms, e.g.

$$\rho u^2 + P - \mu' u_x$$

$$\text{where } \mu' = \rho \Delta x^2 \left| \frac{\partial u}{\partial x} \right|$$

This term is similar to a turbulent Reynolds stress and is of second order accuracy. It also possesses the correct sign to add dissipation to the system.

3. MACCORMACK'S PRESSURE DAMPING (REFERENCE 4)

MacCormack rationalized that boundary layers possess zero normal pressure gradient and therefore an artificial viscosity term proportional to $\frac{\partial^2 p}{\partial n^2}$ will only affect shock waves. His additional damping term is as follows:

$$-\alpha_d \Delta t \Delta x^3 \frac{\partial}{\partial x}\left[\frac{u+c}{4P}\frac{\partial^2 p}{\partial n^2}\right]$$

4. UPWIND DIFFERENCING (REFERENCE 31)

Some differencing schemes possess truncation error terms that behave like artificial viscosity. The upwind differencing method has this feature.

Consider the following model equation:

$$u_t + uu_x = \nu u_{xx}$$

Construct a difference scheme that is central in time, central space, for the diffusion term but upwind for the convective term.

$$\frac{u_i^{n+1} - u_i^{n-1}}{2\Delta t} + u\frac{(u_i^n - u_{i-1}^n)}{\Delta x} = \nu\frac{(u_{i+1}^n - 2u_i^n + u_{i-1}^n)}{\Delta x^2} \quad ; u > 0$$

$$\text{"} \qquad + u\frac{(u_{i+1}^n - u_i^n)}{\Delta x} = \qquad \text{"} \qquad ; u < 0$$

Meteologists used this method and derived the title "upwind" for the direction bias for the one-sided differences.

Let's examine the truncation error based upon the analysis of Hirt.

$$\text{Let } u_i^{n\pm1} = u_i^n \pm \Delta t\, u_t + \frac{\Delta t^2}{2} u_{tt} + \cdots \text{ for time}$$

$$u_{i\pm1}^n = u_i^n \pm \Delta x\, ux + \frac{\Delta x^2}{2} u_{xx} + \cdots \text{for space}$$

Insert these relationships into the difference equation.

$$\text{Hence } U_t + UU_x = \nu U_{xx} \pm U\frac{\Delta x}{2}U_{xx}\ ;\ \begin{matrix}+\text{Upwind}\\ -\text{Downwind}\end{matrix}$$

$$\text{or } U_t + UU_x = \left[\nu + |U|\frac{\Delta x}{2}\right]U_{xx}$$

It is clear than an effective viscosity, ν_e,

$$\text{Where } \nu_e = \nu\left[1 + \frac{|U|\Delta x}{2\nu}\right]$$

is inadvertently added to the governing differential equation by the finite difference process.

In order to obtain an accurate solution it is clear that $\frac{|U|\Delta x}{\nu} < 2$.

SECTION XI

COORDINATE TRANSFORMATION PROCEDURE

Very soon in the study of Computational Aerodynamics one encounters configurations which cannot be described by a Cartesian Coordinate system. Analtic orthogonal coordinate systems exist for a few classic cases, i.e., cylindrical, elliptical, parabolic, spherical, conical, paraboloid, prolate spheroid, oblate spheroid, etc. However, even these cases are certainly limited in application. A more general approach is required to analyze aircraft components. For example, consider an airfoil of arbitrary shape (Reference 48).

Two possible grid systems may be considered: (1) Use a Cartesian grid and establish an interpolation scheme near the surface to describe the boundary condition (Figure 4) or (2) Generate a body-oriented coordinate system and transform the governing equations (Figure 5). The former approach retains the original simple form of the governing equations but over complicates the boundary conditions. In addition, thin viscous layers require clustering of grid points near the surface resulting in further difficulties. The later technique maintains simple boundary conditions but adds more terms to the governing equations. Clustering of points near the surface is readily achieved with a body-oriented system, however, the task of grid generation is an added burden.

All factors considered, the body-oriented system is a clear winner. This method shall now be discussed.

1. BODY-ORIENTED COORDINATES

Consider an arbitrary body-oriented coordinate system (Reference 13)

$$\xi = \xi(x,y)$$

$$\eta = \eta(x,y)$$

where $\eta = 0$ describes the body surface.

The governing equation, $Ex + Fy = 0$, must be transformed into the new coordinates. To accomplish this, the chain rule of differentiation is used.

$$\frac{\partial}{\partial x} = \xi_x \frac{\partial}{\partial \xi} + \eta_x \frac{\partial}{\partial \eta}$$

$$\frac{\partial}{\partial y} = \xi_y \frac{\partial}{\partial \xi} + \eta_y \frac{\partial}{\partial \eta}$$

The Jacobian of the transformation is

$$J = \begin{vmatrix} \xi_x & \eta_x \\ \xi_y & \eta_y \end{vmatrix}$$

The transformed governing equation becomes $(\xi_x E_\xi + \xi_y F_\xi) + (\eta_x E\eta + \eta_y F\eta) = 0$.

It is now apparent that the actual functional form (ξ, η) of the transformation is not required because only the derivative metrics (ξ_x. η_x) appear in the governing equation. This feature facilitates the use of a numerical transformation in which the metrics are computed by finite diffferences. One addition operation is required, however, in order to maintain a simple procedure.

Let's generate the metrics by means of the inverse transformation.

$$x = x(\xi, \eta)$$
$$y = y(\xi, \eta)$$

Then

$$\xi_x = Jy_\eta ; \eta_x = Jy_\xi$$

$$\xi_y = -Jx_\eta ; \eta_y = Jx_\xi$$

and

$$J^{-1} = \begin{vmatrix} x_\xi & y_\xi \\ x_\eta & y_\eta \end{vmatrix}$$

Using the inverse transformation metrics an alternate form for the transformed governing equation becomes

$$J(y_\eta E_\xi - x_\eta F_\xi) + J(-y_\xi E_\eta + x_\xi F_\eta) = 0$$

Dividing by J and manipulating the derivatives produces

$$(y_\eta E - x_\eta F)_\xi + (-y_\xi E + x_\xi F)_\eta$$

$$- E(\overset{\circ}{\cancel{y_{\eta\xi}}} - y_{\xi\eta}) - F(-\overset{\circ}{\cancel{x_{\eta\xi}}} + x_{\xi\eta}) = 0$$

$$\text{or } \hat{E}_\xi + \hat{F}_\eta = 0$$

$$\text{where } \hat{E} = y_\eta E - x_\eta F$$

$$\hat{F} = x_\xi F - y_\xi E$$

The transformed equation is now identical in form to the untransformed equation, however, additional terms have been added to the flux vectors. The main reason for using the inverse transformation is to facilitate the use of numerical derivatives.

Recall that

$$\xi_x = \left.\frac{\partial \xi}{\partial x}\right|_{y=\text{const.}}$$

and

$$x_\xi = \left.\frac{\partial x}{\partial \xi}\right|_{\eta=\text{const.}}$$

The transformed coordinate lines located in physical space readily permit the numerical evaluation of x_ξ but not ξ_x, since lines of constant η have been identified.

$$x_\xi = \left.\frac{\Delta x}{\Delta \xi}\right|_{\eta = \text{const.}}$$

$$y_\eta = \left.\frac{\Delta y}{\Delta \eta}\right|_{\xi = \text{const.}}$$

Hence, the inverse transformation metrics are numerically evaluated from the predetermined grid and inserted into the governing equations.

The only restriction on the transformation is that it be one-to-one (single-valued) and the Jacobian, not vanish in the computational domain. The transformation need not be orthogonal and it is not necessary to evaluate the functional form of the transformation (since only the metrics are required). Also, one need not transform the velocity components which further simplifies the procedure.

Another advantage of this transformation concept is that equal step sizes can be employed in the transformed space which permits the use of simple finite difference operators in the numerical procedure. This is not possible in the interpolation method originally considered as a candidate.

2. CLUSTERING OF GRID POINTS

The use of a transformation permits the contraction of grid points in regions of high gradients. Consider a function E(x) which has large values for the higher derivatives.

The gradient E_x expressed by finite difference is

$$E_x = \frac{E_{i+1} - E_{i-1}}{2\Delta x} - E_{xxx}\frac{\Delta x^2}{6}$$

where $\Delta x = \frac{L}{N}$

N = number of grid points in domain L.

If $E = L\left(\frac{X}{L}\right)^n_n$, then the maximum error in E_x becomes $\left(-Exxx\ \frac{\Delta x^2}{6}\right)_{max} = \frac{n(n-1)\ (n-2)}{-6N^2}$

The percentage error is shown below for various n and for N = 5.

% Error in Ex (N=5)

n	% Error
1	0
2	0
4	-4%
6	-13.3%
11	-60%
16	-140%

Large errors result for high gradients, therefore, one might conclude that more than five grid points are required to reduce the error to an acceptable level. However, another approach would be to stretch the grid in order to achieve smaller gradients in the transformed plane thereby reducing the size of the truncation error term.

Let $\xi = \xi(x)$

$$E_x = \xi_x E_\xi = \xi x\left[\frac{E_{j+1} - E_{j-1}}{2\Delta\xi} - E_{\xi\xi\xi}\frac{\Delta\xi^2}{6}\right]$$

Choosing a stretching factor of the form

$$\xi = L\frac{(X)^m}{L^m}$$

now produces a maximum error in E_x as follows:

$$\left(-\xi_x E_{\xi\xi\xi} \frac{\Delta\xi^2}{6}\right)_{max} = n \frac{\left(\frac{n}{m}-1\right)\left(\frac{n}{m}-2\right)}{6N^2}$$

where $N = \frac{L}{\Delta\xi}$

The percentage error for m = 4 and N = 5 is now within reasonable limits.

n	Transformed % Error
1	-0.87%
2	-0.5%
4	0
6	+0.17%
8	0
11	-0.87%
16	-4%

3. SUMMARY

To expedite the numerical solution of flow fields over arbitrary configurations the equations are transformed into a body-oriented coordinate system. This transformation is accomplished numerically and points are clustered in regions of high gradients to minimize truncation errors. In addition, equal step size is used in the transformed plane to simplify the finite difference operators. Only the independent variables are transformed while the dependent variable velocity components remain oriented to the original (Cartesian) system. (It is not necessary to transform the velocity components unless one desires to eliminate terms through an order of magnitude analysis).

Also, the transformation need not be orthogonal. The resulting transformation adds a few additional terms to the governing equations but greatly improves the accuracy of the method by optimum grid positioning.

The burden of the method is therefore placed upon the Grid Generation procedure which will be discussed next.

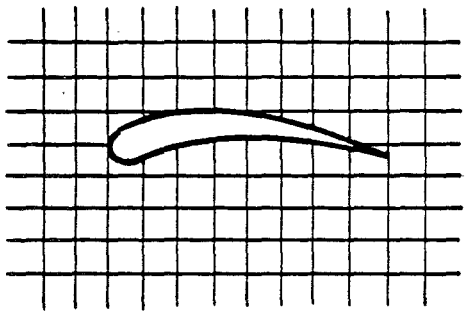

Figure 4. Cartesian Coordinates with Interpolation on Boundary

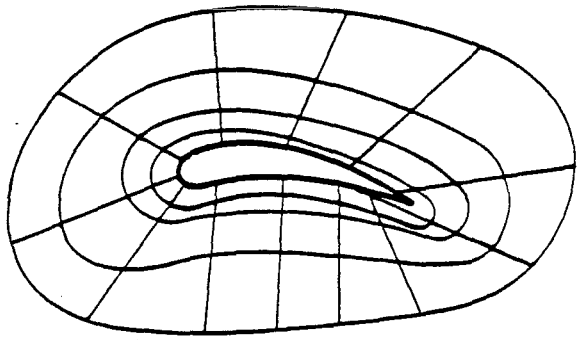

Figure 5. Transformed Body-Oriented Coordinates

SECTION XII

PARABOLIZED NAVIER-STOKES

The complete Navier-Stokes equations offer the potential to solve any problem in fluid dynamics. However, the procedure is the most costly of any prediction method. There is a more efficient solving procedure entitled Parabolized Navier-Stokes (PNS) that can be used under some conditions (Reference 22). These conditions occur for supersonic flow with no streamwise separation (although transverse or cross-flow separation is permissible).

Under this physical situation the elliptic terms in the x-direction (U_{xx}) can be neglected. No downstream information affects this portion of the flow. For this situation, a great mathematical simplification arises and permits the use of PNS.

We shall now explore the development of this method.

Begin with the complete steady Navier-Stokes equations.

$$E_x + F_y + G_z = 0$$

where

$$E = \begin{vmatrix} \rho u \\ \rho u^2 - \sigma_{11} \\ \rho uv - \tau_{12} \\ \rho uw - \tau_{13} \\ \rho ue - u\sigma_{11} - v\tau_{12} - w\tau_{13} - \dot{q}_x \end{vmatrix}$$

All the elliptic terms in the x-direction are contained in the E vector.

$$\tau_{11} = -P + \lambda(\textcircled{u_x} + v_y + w_z) + 2\mu\,\textcircled{u_x}$$

$$\tau_{12} = \mu(u_y + \textcircled{v_x})$$

$$\tau_{13} = \mu(u_z + \textcircled{w_x})$$

$$\dot{q}_x = K\,\textcircled{T_x}$$

By neglecting these first derivative terms in x, we obtain the PNS equations. However, in practice, all viscous terms are dropped in the E vector to simplify the solving procedure. This additional simplification does not greatly limit the method much more than the original assumption of neglecting only the U_{xx} terms.

Hence

$$E = \begin{vmatrix} \rho u \\ \rho u^2 + P \\ \rho uv \\ \rho uw \\ \rho uH \end{vmatrix} = \text{Inviscid}$$

With this formulation it is possible to march in space (x-direction) in a manner similar to marching in time that was previously utilized with the time-dependent Navier-Stokes method. PNS, however, requires up to two order of magnitude less computer time to solve, thereby justifying the approximation.

We shall now demonstrate the method by investigating the flow over a body of revolution traveling at supersonic speeds. The axi-symmetric PNS equations for adiabatic flow follow:

$$E_x + \frac{1}{r}(rF)_r = \tilde{H}$$

where

$$E = \begin{vmatrix} \rho u \\ \rho u^2 + P \\ \rho uv \end{vmatrix} ; \quad a_o^2 = a^2 + \frac{\gamma - 1}{2} u^2$$

$$\tau = \mu(u_r + v_x)$$

$$F = \begin{vmatrix} \sigma v \\ \sigma uv - \tau \\ \sigma v^2 - \sigma_{22} \end{vmatrix} ; \quad \tau_{22} = -P + \lambda \nabla \cdot \underline{V} + 2\mu v_r$$

$$\tau_{\theta\theta} = -P + \lambda \nabla \cdot \underline{V} + 2\mu \frac{v}{r}$$

$$\tilde{H} = \begin{vmatrix} 0 \\ 0 \\ -\sigma_{\theta\theta}/r \end{vmatrix} ; \quad \nabla \cdot \underline{v} = u_x + \frac{1}{r}(rv)_r$$

By using MacCormack's method and marching in x, a new value of the E vector at the next station (x + Δx) is obtained. Resolution of the E vector is required in order to obtain the primitive variables needed in the F and $\tilde{H}$ vectors.

This operation requires further discussion.

$$E_2 = E_1 + \Delta x \left[\tilde{H} - \frac{\partial}{r \partial r}(rF)\right]_1$$

Let

$$E_2 = \begin{vmatrix} \rho u \\ \rho u^2 + P \\ \rho uv \end{vmatrix}_2 \equiv \begin{vmatrix} A \\ B \\ C \end{vmatrix}$$

$$\text{Therefore } v = \frac{\rho uv}{\rho u} = \frac{C}{A}$$

The three remaining relationships with three unknowns ρ, u, P

$$A = \rho u$$

$$B = \rho u^2 + P$$

$$a_o^2 = \frac{\gamma P}{\rho} + \frac{\gamma - 1}{2} u^2$$

can be combined to produce a quadratic equation in any of the variables. The variable selected for resolution is Mach number, M, a combination of all three.

$$\frac{\gamma^2 B^2}{A^2 a_o^2} = \frac{(1+\gamma M^2)^2}{M^2(1+\frac{\gamma-1}{2} M^2)} \equiv \beta^2$$

$$\text{or } M^2 = \frac{\beta^2 - 2\gamma \pm \beta\sqrt{\beta^2 - 2(\gamma+1)}}{2(\gamma^2 - \frac{\gamma-1}{2}\beta^2)}$$

The positive root is supersonic while the negative sign produces a subsonic root. A predicament in this solving scheme arises in that a criteria is necessary to select the correct root. However, a more serious limitation is encountered in that the subsonic root is unstable.

Recall that the original assumption for PNS was supersonic, unseparated flow; therefore only the positive sign on the radical is selected.

$$M^2 = \frac{\beta^2 - 2.8 + \beta\sqrt{\beta^2 - 4.8}}{0.4(9.8 - \beta^2)} \quad \text{for } \gamma = 1.4$$

where $4.8 < \beta^2 < 9.8$ (see Figure 6)

Care must be exercised in selecting the first grid point in the boundary layer to insure that it remains supersonic. (Note: Alternate procedure have been developed to extend the method by setting $\frac{dp}{dn} = 0$ in the boundary layer for $M < 1$ and eliminating the quadratic root).

Once the Mach number is ascertained the primitive variables can be determined.

$$P = \frac{B}{1+\gamma M^2}$$

$$\rho = \frac{\gamma P}{a_o^2}\left(1+\frac{\gamma-1}{2}M^2\right)$$

$$u = \frac{B/A}{(1+1/\gamma M^2)}$$

These values are then updated and the marching procedure continued until the final station is attained.

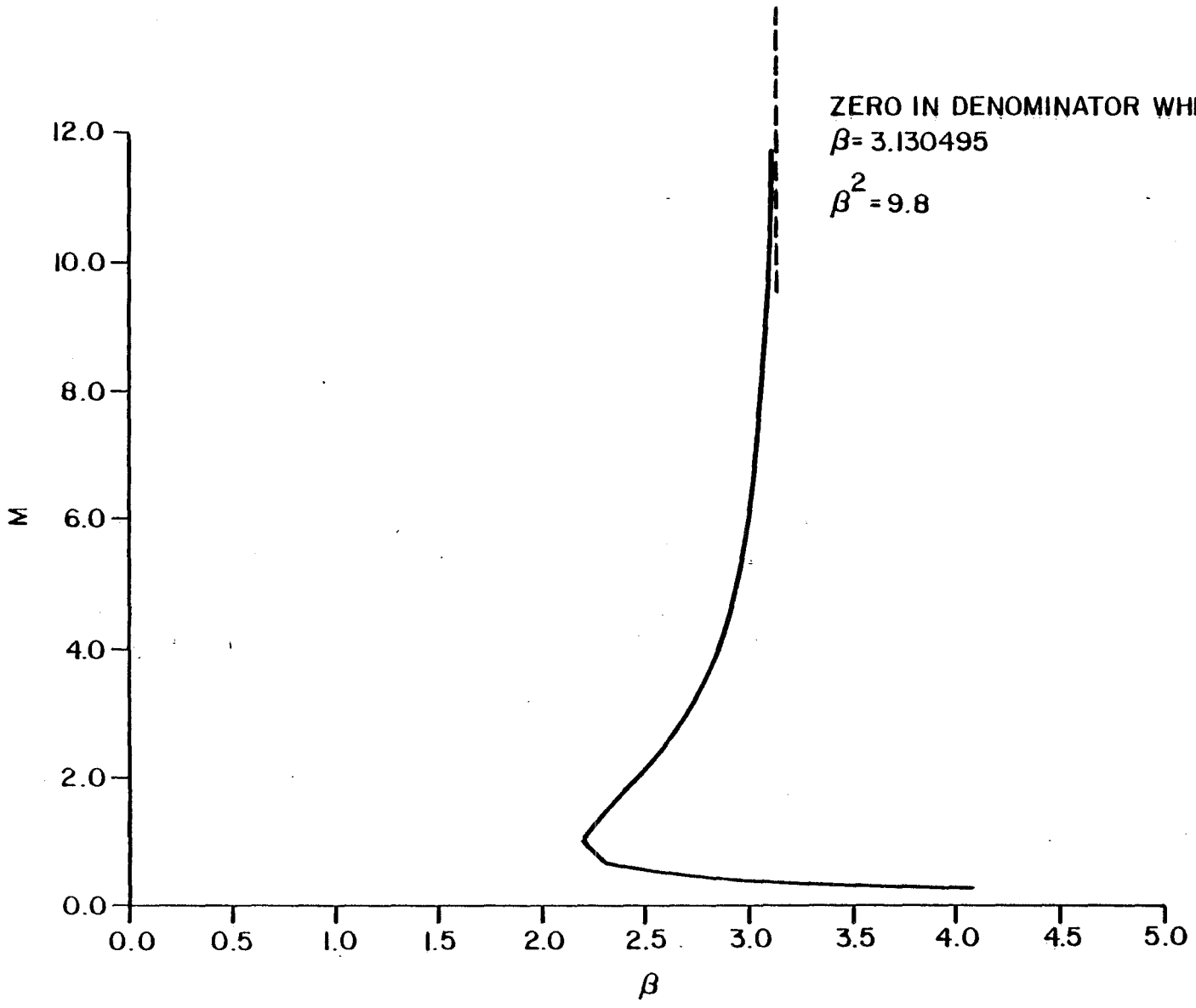

Figure 6. β Versus Mach Number

SECTION XIII

AIR PROPERTIES

Since we will be working with air, a review of its properties is appropriate. In particular, we will require numerical values for the thermodynamic properties and transport properties.

1. THERMODYNAMIC PROPERTIES

Air is a gas mixture composed of about 80% nitrogen and 20% oxygen. Traces of argon, CO_2 and H_2O vapor do not appreciably affect the thermodynamic properties. A gas mixture can be treated as a pure gas provided the properties are evaluated in accordance with the species molecular weight. Shown below is a table of the individual properties of the air components.

TABLE 5

INDIVIDUAL PROPERTIES OF AIR COMPONENTS

Element	Molecular Weight M_i	Concentration C_i	R_i Gas Constant $ft^2/sec^2\ °R$	γ_i
N_2	28.02	.7809	1774	1.404
O_2	32.00	.2095	1552	1.401
A_r	39.94	.0093	1244	1.66

Using these values, the air properties can be determined as follows:

$$\bar{R} = \frac{\Sigma M_i C_i R_i}{\Sigma M_i C_i}$$

For air, the required thermodynamic properties are the following:

Air, M = 28.966, $R = 1716\ ft^2/sec^2{}^\circ R$, $\gamma = 1.40$

$$\text{where } e = C_v T,\ h = C_p T,\ \text{and } p = \rho RT$$

$$\text{and } C_v = \frac{R}{\alpha - 1},\ C_p = \frac{\gamma R}{\gamma - 1}$$

$$\text{since } C_p/C_v = \gamma \text{ and } C_p = R + C_v.$$

These therodynamic properties are the needed values to be used in solving the Navier-Stokes equations in the region where air behaves as a perfect gas. An appreciation for the limits of a perfect gas is required.

2. REAL GAS EFFECTS

As the temperature of a gas is lowered, the phase will change from gas to liquid. Further decrease will solidify the liquid. The temperature values depend upon the pressure level. As the temperature of a diatomic gas is increased above standard sea level conditions, vibrational degrees of freedom arise decreasing γ and accordingly increasing Cv and Cp. Since the molecular weight does not change, R remains constant. This domain is entitled thermally perfect, calorically imperfect. As temperature is further increased, dissociation of the diatomic gas into a monatomic gas occurs. Higher temperatures cause ionization. All these later features produce departures from the perfect gas law. The following is a list of typical temperatures for which the changes occur.

	O_2	N_2
Solidifies	-360°F	-346°F
Liquefies	-297°F	-321°F
Dissociates	5,000°F	10,000°F

These temperature values are well beyond the normal limits encountered in low-speed flight.

However, at hypersonic speeds this is not the case. This can be demonstrated by computing the total temperature for Mach number 10.

$$\frac{T_o}{T_\infty} = 1 + \frac{\gamma - 1}{2} M_\infty^2 = 1 + .2(10)^2 = 21$$

In a wind tunnel a typical value of To is 2100°R. Therefore,

$$T_\infty = 100°R = 360°F$$

Hence, liquefication can be encountered in hypersonic wind tunnels and indeed must be guarded against to avoid erroneous data.

At Mach 10 flight speed, T_∞ = 400°R produces a To = 8400 °R, which clearly dissociates O_2.

To further assist in acquiring an appreciation for the various regions for which real gas effects are encountered (Reference 49) a map of the flight corridor is presented (Figure 7). Note that during reentry both O_2 and N_2 dissociation are encountered. In this range the thermodynamic properties are not constant and hence must be replaced by functional relationships.

use

$\rho = \rho(h,p)$ in place of $\rho = P/RT$

$e = e(h,p)$ in place of $e = C_v T$

$T = T(h,p)$ in place of $T = h/C_p$

In the governing equations, h and p are computed and interpolation tables used to obtain ρ, e and T. In addition, the $\dot{q}$ term must include the heat of dissociation to account for recombination heating on the surface. The net result, however, is that perfect gas heating is nearly equal to real gas heating due to the fact that Lewis number is near unity implying that the heat transfer by diffusion is almost the same as by conduction. Real gas effects merely redistribute the modes of heat transfer without changing the total amount.

3. TRANSPORT PROPERTIES

Three transport properties exist which account for the transport of mass, momentum and energy throughout the gas. The relationship for these three modes of transport are as follows:

$$\text{Mass: } \dot{m}_i = \rho D \frac{\partial C_i}{\partial n}\ ;\ D = \text{diffusion coefficient (Fick's law)}$$

$$\text{Momentum: } \tau = \mu \frac{\partial V}{\partial n}\ ;\ \mu = \text{viscosity (Stokes law)}$$

$$\text{Energy: } \dot{q} = k \frac{\partial T}{\partial n}\ ;\ k = \text{conductivity (Fourier law)}$$

To solve problems in fluid mechanics numerical values of these three transport properties are required. However, in practice one value is prescribed (μ) while the combinations of others is given (k and D).

Certain combinations of these coefficients occur naturally in the governing equations and have been given labels. For example,

$$\frac{\dot{Q}(\text{dissipation})}{\dot{Q}(\text{conduction})} = \frac{\tau V}{kT/L} = \frac{\mu V^2/L}{kT/L} = \frac{\mu Cp}{k}\left(\frac{V^2}{Cp\bar{T}}\right)$$

$$\text{where } P_r = \frac{\mu Cp}{k} = \text{Prandtl Number};\ M^2 = \frac{2}{\gamma - 1}\left(\frac{V^2}{Cp\bar{T}}\right) = \text{Mach Number}$$

$$\text{Also } \frac{\dot{Q}(\text{diffusion})}{\dot{Q}(\text{conduction})} = \frac{m_i \Delta h}{kT/L} = \frac{\rho D \Delta h Ci/L}{kT/L} = \frac{\rho DCp}{k}\left(\frac{Ci\Delta h}{CpT}\right)$$

where

$$(\text{Lewis Number}) = L_e = \frac{\rho DCp}{k}$$

Hence, three transport properties may be entrered into the governing equations as follows:

$$\mu = (2.27 \times 10^{-8}) \frac{T^{3/2}}{T + 198.6°R} \quad \frac{lb\ sec}{ft^2} \quad \text{Sutherland's Law}$$

$$P_r = \frac{\mu C_p}{k} = .72$$

$$L_e = \frac{\rho D C_p}{k} = 1.4$$

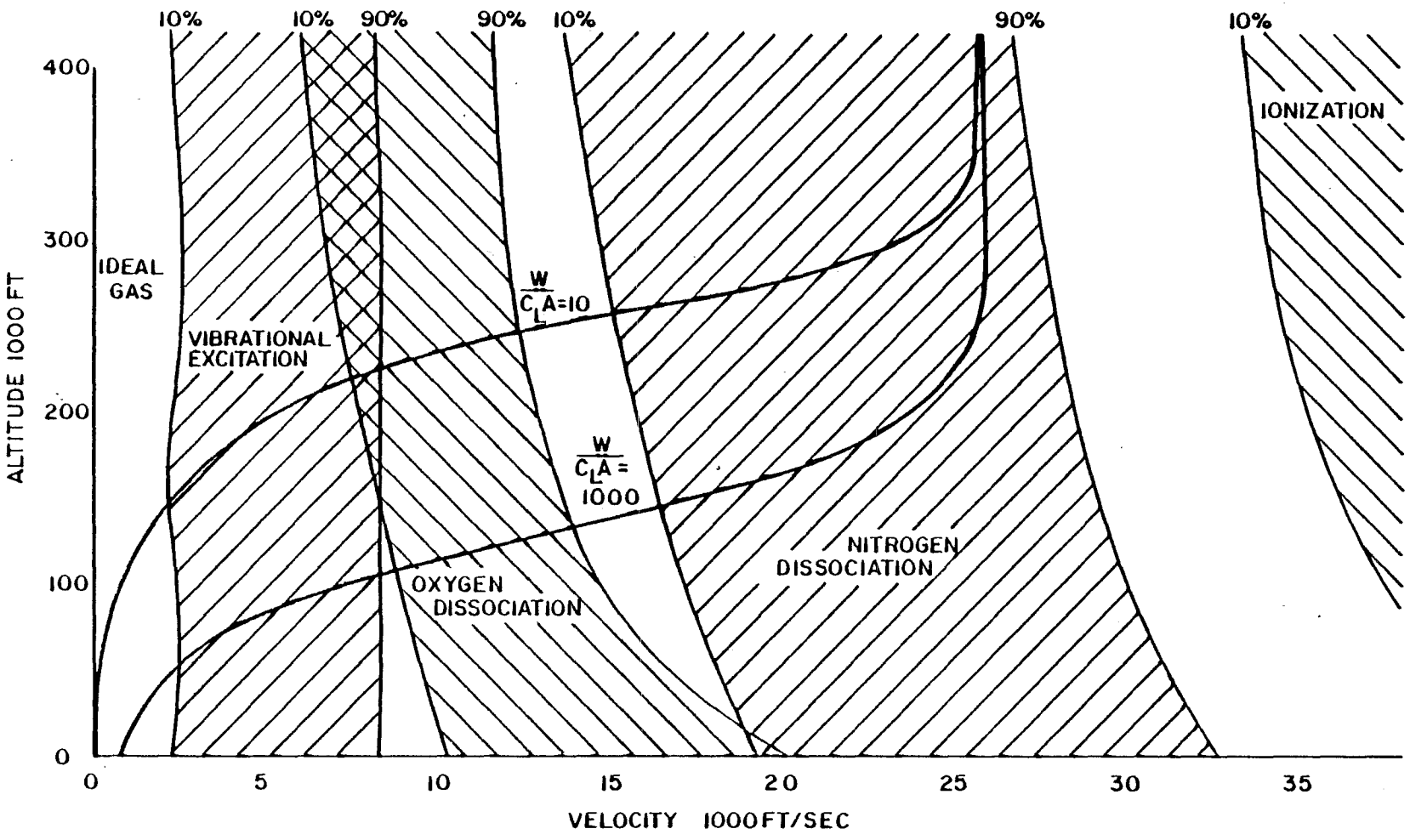

Figure 7. Zones of Energy Excitation

SECTION XIV

BOUNDARY CONDITIONS

The importance of the boundary conditions in solving partial differential equation can hardly be overstated (Reference 50). This is apparent if you note that the only difference in formulation between any two vastly different flow problems is the location and value of the boundary conditions since the same Navier-Stokes equations govern the interior regions for all fluid flow problems.

In this section, various boundary conditions will be explored. First, the type of boundary conditions will be classified (References 51, 52 and 53).

a) Dirichlet, in which the value of the function is specified; u=a.

b) Neumann, in which the normal gradient of the function is specified. $U_y = b$

c) Mixed (Robbins), which is a combination of the above two types.

$$U + bU_y = c$$

The behavior of the solution depends upon the type of boundary conditions applied.

Next we consider the location of the boundary conditions, i.e., either on a body surface boundary or at a far field boundary sufficiently removed from the body under investigation. The former is normally well defined geometrically while the later possesses some arbitrary features which must be defined by the computational aerodynamicist. The body and far field boundary conditions will now be discussed separately.

1. SURFACE BOUNDARY CONDITIONS

On the surface the velocity and temperature must be prescribed. For a viscous fluid, a no slip condition is appropriate with no flow through the surface. (Although small amounts of bleed or suction can be considered readily).

$$\underline{V}(\eta=0)=0$$

$$\text{or } u,v,w(\eta=0)=0$$

Normally, on the surface either a prescribed wall temperature or prescribed temperature gradient is used.

$$T(\eta=0)=Tw$$

$$\text{or } \frac{\partial T}{\partial \eta}(\eta=0)=0 \text{ Adiabatic}$$

More complex relationships are possible through consideration of the heat transfer process.

Frequently the wall temperature will not be known so that an estimate must be made. Consider the heat energy balance within a small surface element.

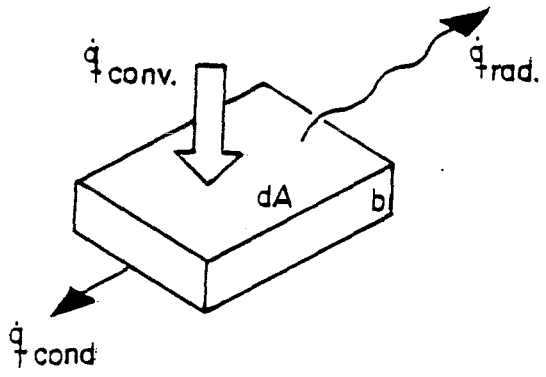

The net heat into the element is obtained through consideration of convection, conduction and radiation. This net heat input will increase the thermal energy of the element. (Note, under some circumstances, additional forms of heat energy must also be considered, i.e., ablation, evaporation, sublimation, change of phase, etc.)

Heat Balance

$$(\dot{q}_{conv} - \dot{q}_{cond} - \dot{q}_{rad})dA = C_m \dot{T}\, dm$$

or

$$h(Taw - \dot{T}w) - \frac{Km}{b}(\dot{T}w - Ti) - \epsilon\sigma(\dot{T}w^4 - Tr^4) = \rho_m \Delta b\, C_m \dot{T}w$$

All forms of heat exchange conceptually can be grouped into the following form:

$$\bar{h}(Ta - \dot{T}w) = \rho_m b C_m \dot{T}w$$

or

$$\frac{\dot{T}w}{Ta - \dot{T}w} = \frac{\bar{h}}{\rho_m b C_m} \equiv \frac{1}{\tau}$$

where τ is the time constant for the element to attain equilibrium temperature.

For convection dominated problems

$$\tau = \frac{\rho_m b C_m}{\rho V C_p} \quad \text{and} \quad Ta = Taw$$

For a thin skin steel model in a supersonic tunnel, τ is about a minute. Therefore, adiabatic wall temperature will be attained in a continuous flow tunnel. However, for an impulse tunnel with running times in the millisecond range, room temperature is the appropriate value for the wall.

For flight application above M=3 the radiation energy exchange becomes important and a "radiation equilibrium temperature" is attained.

$$\dot{q}_{conv} = \dot{q}_{rad} \quad \text{as } \dot{T} \to 0$$

$$h(Taw - \dot{T}w) = \epsilon\sigma Tw^4$$

$$\text{or } \dot{T}w = \frac{Taw}{1 + \epsilon\sigma Tw^3/h}$$

For this case Tw is less than Taw.

Estimates, similar to these, are generally acceptable for the determination of the wall temperature boundary conditions to be used in solving the Navier-Stokes equations. Fortunately, the pressure coefficient, skin friction and heat transfer coefficients are not extremely sensitive to the value of the wall temperature. Listed below are the dimensionless relationships for a laminar boundary layer under zero pressure gradient for different wall temperature (Reference 54).

T_w/T_{aw}	$C_f/\sqrt{2Re}$	$2St/\sqrt{2Re}$	$\frac{\delta^*}{\theta}$ tr
1.0	.46960	.46960	2.591
0.8	"	"	2.073
0.6	"	"	1.555
0.4	"	"	1.036
0.2	"	"	0.518
0	"	"	0

One additional point must be addressed concerning surface boundary conditions. Although no wall boundary conditions on either p or ρ are required for solving the differential equations, values for both are needed on the surface for the numerical central difference scheme.

To accomplish this, one of the governing equations evaluated at the wall may be utilized. The normal momentum equation is selected for this purpose. The resulting condition is called a "compatibility relationship" and should not be called a boundary condition (although frequently mislabeled in the literature).

$$\rho(V_t + \cancelto{0}{UV_x} + VV_y)_{y=0} + (P_y - \tau_x)_{y=0} = 0$$

$$\text{or } P_y = \tau_x$$

However, since $P >> \tau$ and $\frac{\partial}{\partial y} >> \frac{\partial}{\partial x}$ a simple compatibility condition results, accuarate to order Re^{-1}, for the determination of wall pressure.

$$\left.\frac{\partial p}{\partial \eta}\right|_{\eta=0} = 0$$

Density is then obtained from the equation of state.

$$\rho_w = \frac{P_w}{R\,T_w}$$

This completes the description of surface boundary conditions.

2. FAR FIELD BOUNDARY CONDITIONS

As stated previously, the specification of the far field boundary conditions depends upon whether the flow is subsonic or supersonic. This section is intended to provide some insight into the description of the outer boundary conditions for the different flow classes (Reference 55).

To establish this insight, let us first consider the boundary conditions for the simple wave equation.

$$\frac{\partial u}{\partial t} + c\frac{\partial u}{\partial x} = 0$$

The general solution of this equation is $u = u(x-ct)$

In the wave diagram for this flow, signals are propagated at speed c and therefore boundary condition information is also propagated at $\frac{dx}{dt} = c$.

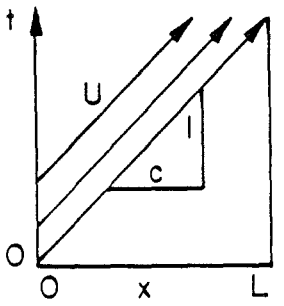

$$U_t + cU_x = 0$$

It is clear that in this case, only one boundary condition on x can be applied and must be applied at the upstream end to properly pose the problem, i.e., u(o, t). Initial conditions are also required; u (x,o).

It is also clear that if c < 0 the waves propagate in the opposite direction.

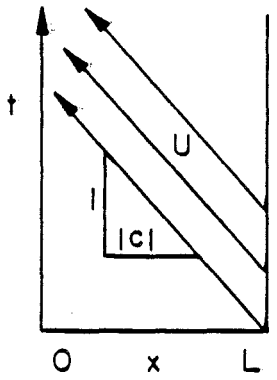

$$U_t - |c| U_x = 0$$

Again in this case, only one boundary condition in x is required but must be applied at the downstream end, i.e., u (L, t).

Next consider a two equation system.

$$U_t + cU_x = 0$$

$$V_t - aV_x = 0$$

For this system, it is obvious that the boundary condition on u be placed at x=0, while the boundary condition on v should be placed at x = L. A set of initial conditions must also be provided for both u and v. In this form u and v are called the characteristic variables and propagated at speed c and -a respectively.

If we could find the characteristic variables for the fluid dynamic equations, this would provide necessary information to help describe the boundary conditions.

To accomplish this, let's consider the one-dimensional Euler equations. For most problems the viscous effects are minor near the outer boundary and therefore, the inviscid equations are appropriate.

$$\begin{vmatrix} \rho \\ \rho u \\ \rho e \end{vmatrix}_t + \begin{vmatrix} \rho u \\ \rho u^2 + p \\ \rho u H \end{vmatrix}_x = 0$$

$$\text{where } H = e + P/\rho = \frac{a^2}{\gamma - 1} + \frac{u^2}{2}$$

These equations can be rearranged into the following form:

$$\frac{D\pi}{Dt} + u_x = 0$$

$$\frac{Du}{Dt} + a^2 \pi_x = 0$$

$$\frac{D}{Dt}(\pi - R) = 0$$

$$\text{where } \pi = \frac{1}{\gamma} \ln p$$

$$R = \ln \rho$$

$$a^2 = \frac{\gamma p}{\rho}$$

The equations are exact but non-linear. To obtain the characteristic variables we must assume small perturbations and linearize the set. Again, near the far field boundary this assumption does not lead to a serious restriction.

Now let

$$q = u + \pi a_1$$

$$r = u - \pi a_1$$

$$s = \pi - R \text{ (entropy)}$$

Therefore, the inverse relationship are the following:

$$\pi = \frac{q-r}{2a_1}$$

$$R = -s + \pi$$

$$u = \frac{q+r}{2}$$

In the new variables, the three linearized equations become

$$q_t + (u_1 + a_1) q_x = 0$$

$$r_t + (u_1 - a_1) r_x = 0$$

$$s_t + (u_1) s_x = 0$$

The characteristic variables are then q, r and s which propagate at speeds $u_1 + a_1$, $u_1 - a_1$ and u_1 respectively.

It is also apparent that q and s will always have positive propagation speed, ($u_1 > 0$ conventionally defined in freestream direction) and therefore must be prescribed at the upstream boundary.

The variable r possesses either positive or negative propagation speed depending upon whether the flow is supersonic or subsonic, respectively.

Therefore, r is prescribed at the upstream boundary if $\frac{u}{a} > 1$ and at the downstream boundary if $\frac{u}{a} < 1$.

These three boundary conditions are appropriate for one-dimensional unsteady flow and no additional ones are needed or permitted. The numerical system generally needs additional information on the boundaries due to the manner in which the finite difference operators are constructed. In this case "compatibility conditions" are used to resolve this predicament and should not be confused with valid boundary conditions. The "compatibility conditions" add no new information but merely redescribe the available information, e.g., insuring that the governing equations are satisfied at the boundary. For the one-dimensional Euler equations, we will merely

reuse the characteristic equations at the boundary to resolve the undefined variables. Below is a summary of the appropriate boundary conditions for either supersonic or subsonic flow.

3. SUMMARY ONE-DIMENSIONAL FLOW

Far Field Boundary Conditions

Subsonic

$x_1 = 0$	$x_2 = L$
$q = q_1$	$\left[q_t + (u+a) q_x\right]_2 = 0$
$\left[r_t + (u-a) r_x\right]_1 = 0$	$r = r_2$
$s = s_1$	$\left[s_t + (u) s_x\right]_2 = 0$

Supersonic

$x_1 = 0$	$x_2 = L$
$q = q_1$	$\left[q_t + (u+a) q_x\right]_2 = 0$
$r = r_1$	$\left[r_t + (u-a) r_x\right]_2 = 0$
$s = s_1$	$\left[s_t + (u) s_x\right]_2 = 0$

The following figures show the implementation of these boundary conditions for the Navier-Stokes equations for $M_\infty = 0.5$ uniform flow state.

Initially a square wave is inserted into the middle of the flow field and Figures 8 and 9 show the propagation of the characteristic variables (q, r,s) at different time levels. These are the correct boundary conditions in this case and no reflections at the boundary occur. In Figure 10 a case is displayed for the inappropriate boundary conditions (but commonly employed) of ρ_∞, U_∞, P_∞ given upstream and ρ_x, U_x, P_x downstream. Note in

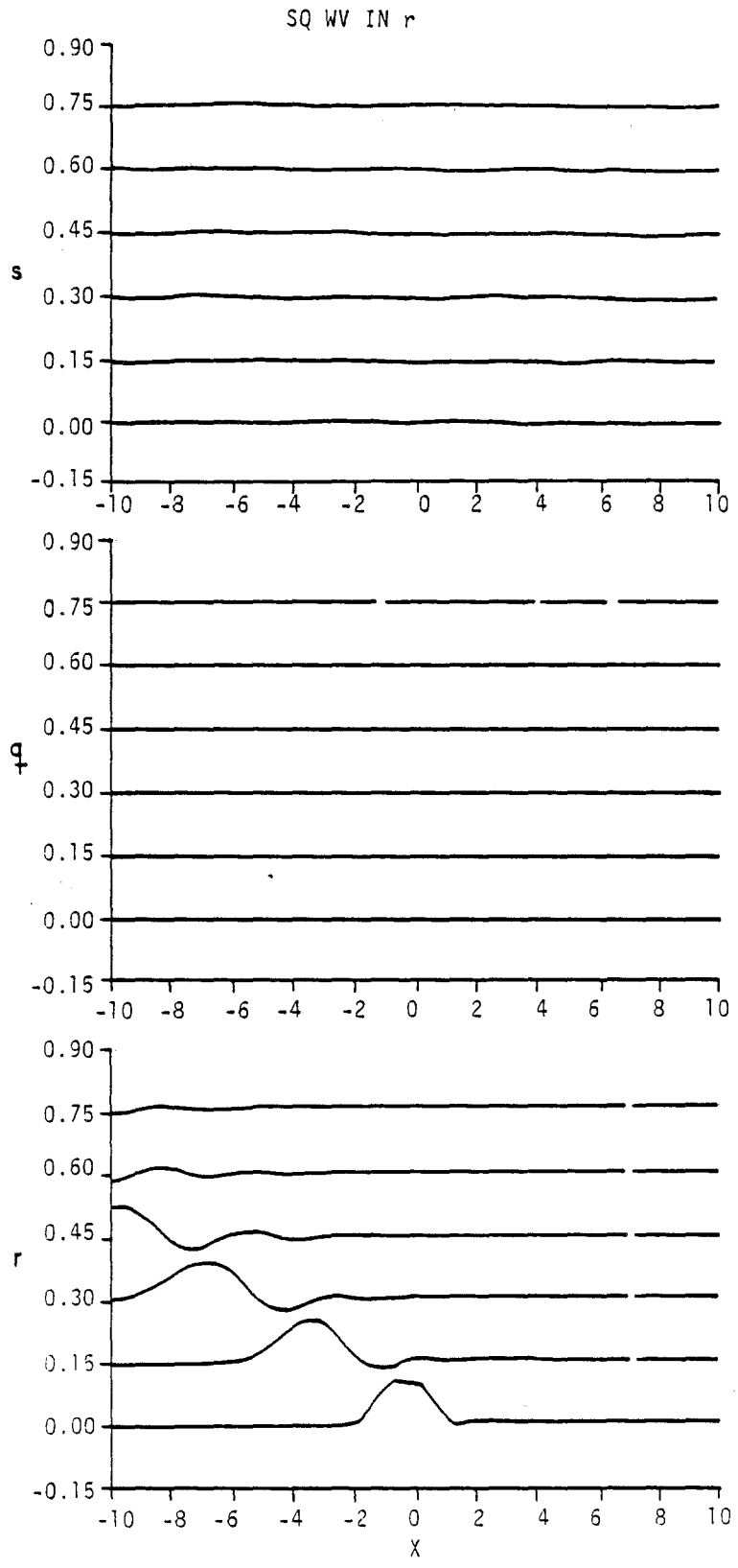

$M_\infty = 0.5$ q_1, s_1, r_2 given

Figure 8. Wave Diagram for Square Wave Input

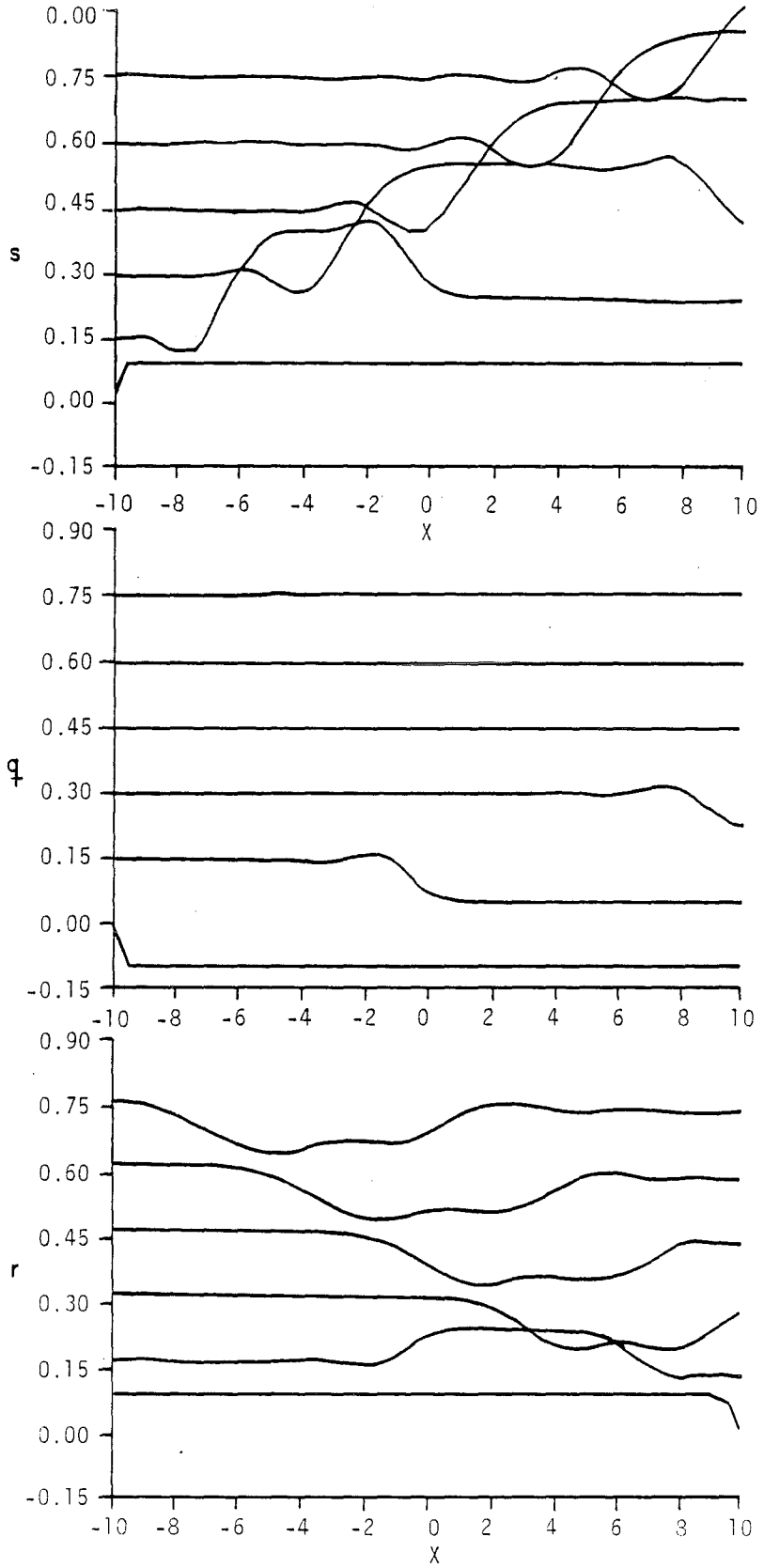

Figure 9. Wave Diagram for Initial Condition Disturbances (Correct Boundary Conditions)

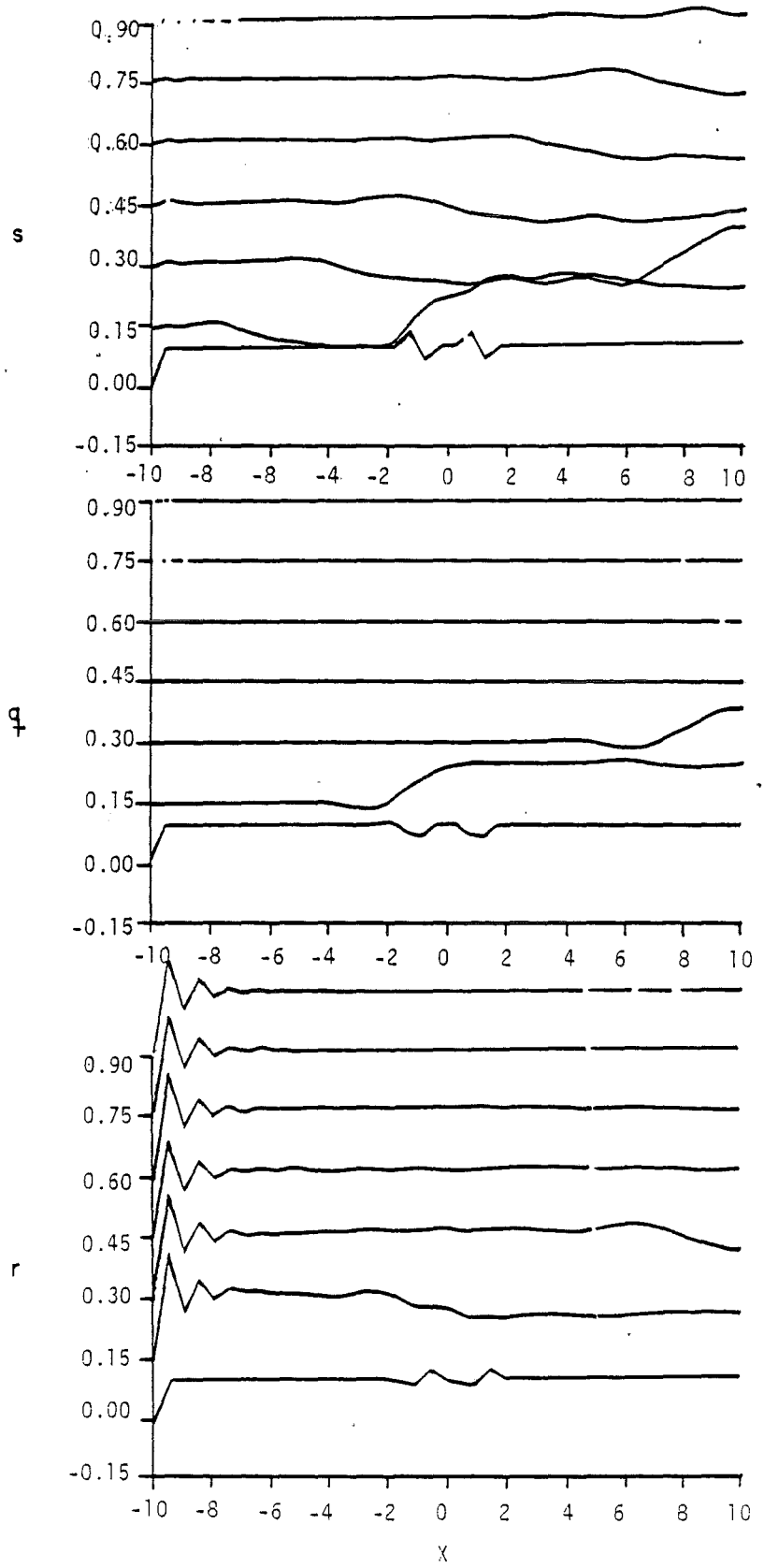

Figure 10. Wave Diagram for Initial Condition Disturbances (Incorrect Boundary Conditions)

this case that waves continue to reflect from the boundaries resulting in large errors.

4. BRANCH CUT BOUNDARY CONDITIONS

Frequently within the computational domain a branch cut is inserted which joins the inner and outer boundaries dividing the flow field into separate sections. For example, for symmetrical configurations a branch cut is located on the plane of symmetry which permits one to solve only one-half of the problem, thereby saving one-half of the computer resources. Along these branch cuts boundary conditions must be applied. Two types occur, i.e., symmetric and periodic.

5. SYMMETRY PLANE

For this situation, no flow is permitted through the plane and all gradients normal to the plane must vanish

$$v=0 \text{ and } \frac{\partial U}{\partial n}=0$$

6. PERIODIC CONDITIONS

For the case of an arbitrary artificial boundary located in the field, for example, encountered in a cascade of turbine blades, all properties must be continued across the cut. Due to the periodic nature of this situation the following boundary condition is appropriate

$$U_1=U_N$$

Where stations 1 and N in the transformed plane are geometrically coincident stations in the physical plane representing the multivalued features of the configuration.

7. CLASSIFICATION OF PARTIAL DIFFERENTIAL EQUATIONS

Non-linear partial differential equations can be classified according to the type of subsidiary condition that must be imposed to give a well-posed problem. Consider a non-linear, second order quasi-linear partial differential equation.

$$A\frac{\partial^2 u}{\partial x^2} + 2B\frac{\partial^2 u}{\partial x \partial y} + C\frac{\partial^2 u}{\partial y^2} = \Phi(u, ux, uy, x, y)$$

where A,B,C = functions of x, y only

Also assumed valid in the x,y plane are the total derivative definitions.

$$dux = \frac{\partial}{\partial x}(ux)dx + \frac{\partial}{\partial y}(ux)dy$$

$$duy = \frac{\partial}{\partial x}(uy)dx + \frac{\partial}{\partial y}(uy)dy$$

This constitutes three equations for the determination of u_{xx}, u_{xy} and u_{yy}.

$$\text{Determinant} = D = \begin{vmatrix} A & 2B & C \\ dx & dy & 0 \\ 0 & dx & dy \end{vmatrix}$$

Two families of characteristics (real or complex conjugates) curves exist on which D=0. This relation is known as the equation of characteristics.

$$Ady^2 - 2Bdxdy + Cdx^2 = 0$$

$$\text{or } \left|\frac{dy}{dx}\right|_{\mu} = \frac{B \pm \sqrt{B^2 - AC}}{A}$$

Three classes of equations have been identified dependent upon the condition of the radical (Reference 5

1. Elliptic $B^2 - AC < 0$

   The characteristics are complex conjugates

2. Parabolic $B^2 - AC = 0$

   Only one real family of characteristics exist.

3. Hyperbolic $B^2 - AC > 0$

   Characteristic are real

Examples of the three classes are as follows:

1. Laplace Equation for two-dimensional flow.

$$\frac{\partial^2 \phi}{\partial x^2} + \frac{\partial^2 \phi}{\partial y^2} = 0$$

$A=1$

$B=0 \quad B^2 - AC = -1 < 0$ Elliptical

$C=1 \quad \frac{dy}{dx} = \pm i$

2. Heat conduction in thermodynamics

$$\frac{\partial T}{\partial t} - \alpha \frac{\partial^2 T}{\partial x^2} = 0$$

$A=0$

$B=0 \quad B^2 - AC = 0$ Parabolic

$C=-\alpha \quad \frac{\partial x}{\partial t} = 0$

3. Vibrating string in mechanics.

$$\frac{\partial^2 y}{\partial t^2} - a^2 \frac{\partial^2 y}{\partial x^2} = 0$$

$A=1$

$B=0 \quad B^2 - AC = a^2 > 0$ Hyperbolic

$C=-a^2, \frac{dx}{dt} = \pm a$

The description of the outer boundary conditions for flow fields is quite different depending upon the classification of the type of partial differential equations.

SECTION XV

GRID GENERATION PROCEDURE

An automated procedure is needed to generate a body-oriented coordinate system for arbitrary geometries. Three types shall be discussed, i.e., algebraic, elliptic and hyperbolic; which are typical of the types presently in use. This is an area, however, where improvements are required in order to upgrade the overall efficiency of computational aerodynamics.

1. ALGEBRAIC METHOD

The homotropy method of R. Smith (Reference 55) is an example of an algebraic method. In this approach, geometric-constructs are used to define a grid without resort to differential equations. First, define the body contour with grid points located at constant increments of arc length (Figure 11). Label this curve η=0. Next, construct an outer boundary with the same number of grid points as on the body and also at constant increments of arc length. Label this curve η=N. These two curves need not be of equal arc length but they must possess the same number of grid points. Now connect the first point of the η=0 curve with a straight line to the first point of the η=N curve. Next, sequentially connect all the points between the two curves with straight lines. Label these straight lines ξ = 0, 1, 2 ...M in numerical sequence. Now divide all ξ lines into N steps of similar proportion. Any proportion is feasible although a systematic regular variation produces the best results. (This maintains better behavior of the higher derivatives of the metrics). Now connect these points to form the family of η = constant curves. From this constructed network a one-to-one relationship of $x(\xi,\eta)$ and $y(\xi,\eta)$ can be determined for which the metrics can be computed numerically. An example of this grid is shown in Figure 12.

2. ELLIPTIC METHOD

The pioneering method of J. Thompson (Reference 57) in the use of a general transformation procedure was responsible for early successes in the field. This procedure (Reference 46) also involves establishing an inner body contour (η=N). On these contours a grouping of (x,y) points is selected to define a closed contour; C_1 (x,y) on the inner and C_2(x,y) on the outer contour (Figure 13)

A simple mapping is desired to determine the interior points with constraints that a minimum or maximum not occur in the interior (to maintain single-valuedness) and also that coordinate lines of the same family not intersect. The elliptic Laplace equation contains these desired features.

$$\nabla^2 \eta = 0 = \eta_{xx} + \eta_{yy}$$

This equation with boundary conditions on C_1 and C_2 completely define the problem.

A second family is also generated by the Laplacian with periodic boundary conditions at an arbitrary branch cut.

$$\nabla^2 \xi = 0$$

To solve these equations we resort to the inverse transformation and exchange dependent and independent variables. It will be seen that numerical solution in the transformed plane is more convenient.

The chain rule states that

$$\frac{\partial}{\partial x} = \xi_x \frac{\partial}{\partial \xi} + \eta_x \frac{\partial}{\partial \eta}$$

$$\frac{\partial}{\partial y} = \xi_y \frac{\partial}{\partial \xi} + \eta_y \frac{\partial}{\partial \eta}$$

where

$$\xi_x = J^{-1} y_\eta \qquad \xi_y = -J^{-1} x_\eta$$

$$\eta_x = -J^{-1} y_\xi \qquad \eta_y = J^{-1} x_\xi$$

$$J = x_\xi y_\eta - x_\eta y_\xi$$

Applying the inverse transformation to the Laplacian equation produces the following:

$$J^2 \nabla^2 \xi = (y_\eta y_{\eta\xi} - y_\eta y_{\eta\eta} + x_\eta x_{\eta\xi} - x_\xi x_{\eta\eta})$$

$$-\alpha J^{-1} J_\xi + \beta J^{-1} J_\eta$$

and

$$J^2 \nabla^2 \eta = (-y_\eta y_{\xi\xi} + y_\xi y_{\xi\eta} - x_\eta x_{\xi\xi} + x_\xi x_{\xi\eta}) + \beta J^{-1} J_\xi - \gamma J^{-1} J_\eta$$

where

$$\alpha = x_\eta^2 + y_\eta^2$$

$$\beta = x_\xi x_\eta + y_\xi y_\eta$$

$$\gamma = x_\xi^2 + y_\xi^2$$

Combining these relationships produces the transformed Laplacian for x and y.

$$-J^2(x_\xi \nabla^2 \xi + x_\eta \nabla^2 \eta) = 0 = \alpha x_{\xi\xi} - 2\beta x_{\xi\eta} + \gamma x_{\eta\eta}$$

$$-J^2(y_\xi \nabla^2 \xi + y_\eta \nabla^2 \eta) = 0 = \alpha y_{\xi\xi} - 2\beta y_{\xi\eta} + \gamma y_{\eta\eta}$$

These two sets of coupled elliptic partial differential equations require numerical solution. Two methods have been used, i.e. SOR (successive-over-relation) and ADI (alternating direction implicit method).

3. SOR SOLVER

The method of successive-over-relaxation (SOR) was developed by Young (1954). It is an iteration method to relax the equation from some initial guess by driving the error residuals to zero at each point. The term "over-relaxing" implies applying a larger correction than the standard relaxation calculation produces in order to accelerate convergence.

To demonstrate the procedure consider the original Laplace equation.

$$\nabla^2 \xi = 0$$

In finite differences it becomes

$$\frac{\xi_{i+1,j} - 2\xi_{i,j} + \xi_{i-1,j}}{\Delta x^2} + \frac{\xi_{i,j+1} - 2\xi_{i,j} + \xi_{i,j-1}}{\Delta x^2} = 0$$

If $\Delta x = \Delta y$ for simplicity, then at any iteration cycle the residual becomes

$$r_{ij} = \left[\xi_{i+1,j} + \xi_{i-1,j} + \xi_{i,j+1} + \xi_{i,j-1} - 4\xi_{i,j}\right]$$

These residuals are calculated at each point in the field. Corrections are then applied in a systematic fashion for the next iteration. Various methods have been developed to improve convergence. SOR uses the following:

$$\xi_{i,j}^{n+1} = \xi_{i,j}^{n} + \frac{\omega}{4} r_{i,j}^{n}$$

where n = iteration level

$$1 \leq \omega \leq 2 = \text{relaxation factor}$$

The method is continued until the residuals are driven to sufficiently small valves.

4. ADI SOLVER

The alternating direction implicit method (ADI) was introduced by Peaceman and Rachford (1955) (Reference 31). The method splits the equations into two one-dimensional parts and uses the efficient tridiagonal solver in each direction alternatively (References 58 and 59). First. sweep in one direction while holding the derivatives constant in the other and then reverse the procedure to complete the cycle.

Step 1

$$\xi_{i+1,j}^{n+1/2} - 2\xi_{i,j}^{n+1/2} + \xi_{i-1,j}^{n+1/2} = -\Delta x^2 \left(\frac{\partial^2 \xi}{\partial y^2}\right)^n$$

Step 2

$$\xi_{i,j+1}^{n+1} - 2\xi_{i,j}^{n+1} + \xi_{i,j-1}^{n+1} = -\Delta y^2 \left(\frac{\partial^2 \xi}{\partial x^2}\right)^{n+1/2}$$

Again, the alternative sweeps are continued until convergence is achieved.

5. HYPERBOLIC METHOD

In external aerodynamics, the location of the outer boundary need not be specified; it only need be far removed from the inner boundary. Hyperbolic methods (Reference 5) may be used in this case as developed by J. Steger (1980). We seek a grid composed of constant ξ and η lines given initial data along $\eta = 0$ on the body contour. A set of partial

differential equations are sought to generate a smoothly varying mesh such that grid lines of the same family do not intersect or coalese. These equations may be obtained from two conditions, i.e. an orthogonality condition and a geometric constraint..

$$x_\xi x_\eta + y_\xi y_\eta = 0 \qquad \text{(Cauchy-Riemann) Orthogonality Condition}$$

$$x_\xi y_\eta - x_\eta y_\xi = J(\eta) \quad = \text{Area Constraint}$$

Cramer's Rule may be used to solve for x_η and y_η

$$x_\eta = \frac{-J y_\xi}{x_\xi^2 + y_\xi^2} = \frac{\begin{vmatrix} 0 & y_\xi \\ J & x_\xi \end{vmatrix}}{\begin{vmatrix} x_\xi & y_\xi \\ -y_\xi & x_\xi \end{vmatrix}}$$

$$y_\eta = \frac{J x_\xi}{x_\xi^2 + y_\xi^2}$$

These equations are hyperbolic and can be marched in the η direction.

The advantages of the method is that it is fast, orthogonal, automated and clustering can be controlled by varying J. It can only be used, however, when the outer boundary need not be specified (Figure 14).

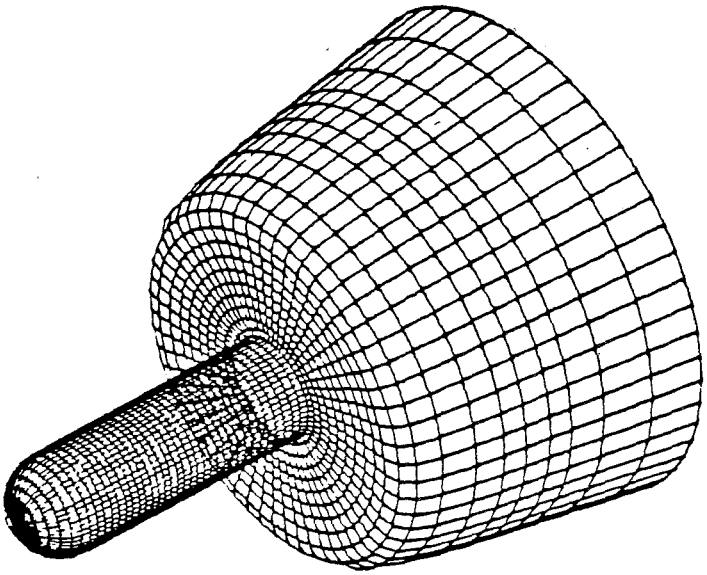

Figure 11. Surface for Spike-nosed Body

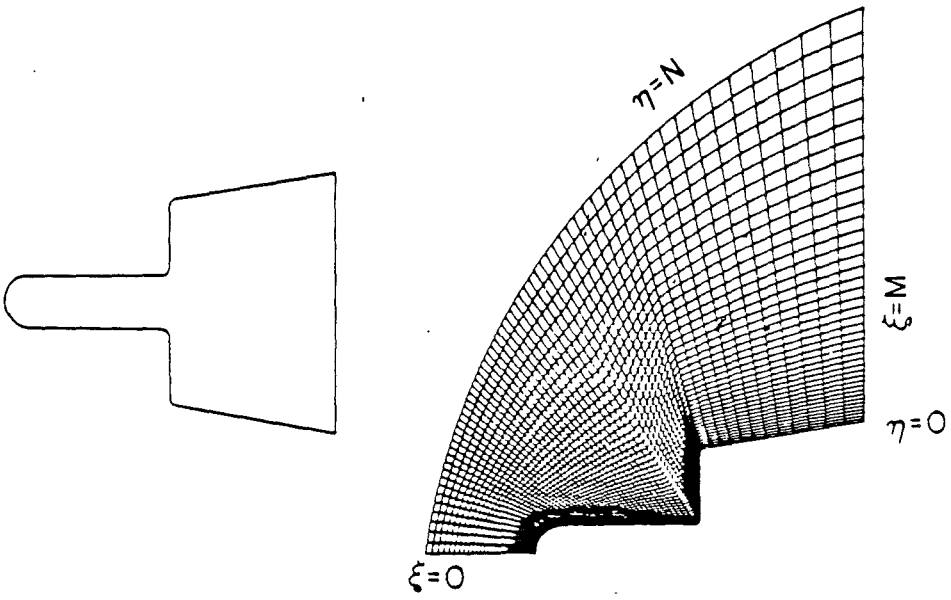

Figure 12. Flow Field Mesh for Spike-nosed Body

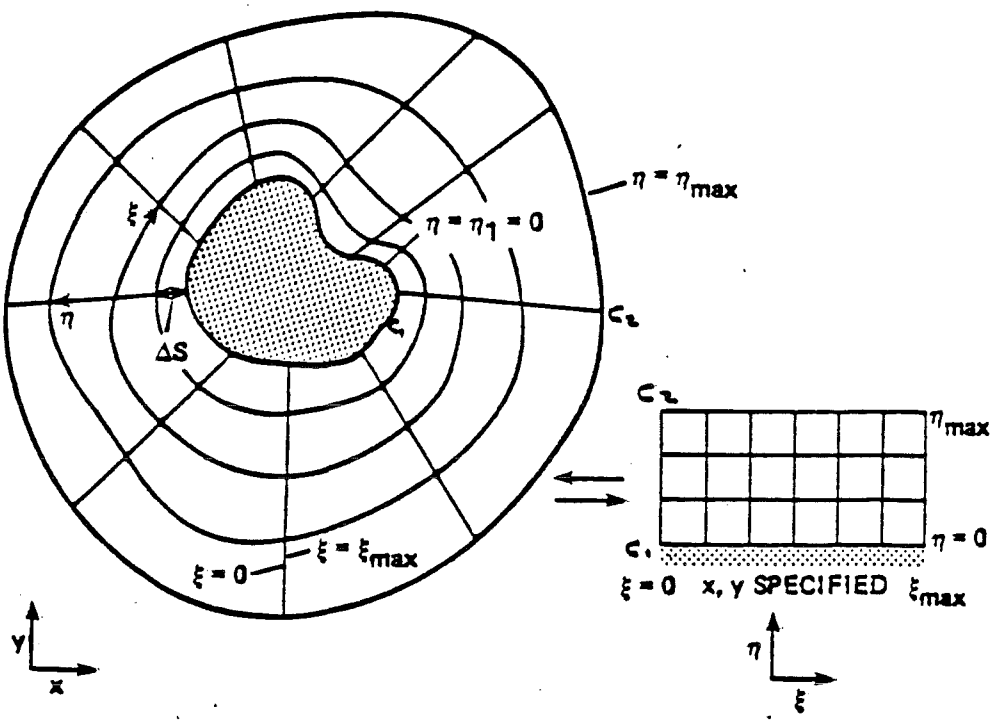

Figure 13. Sketch of Physical and Computational Plane

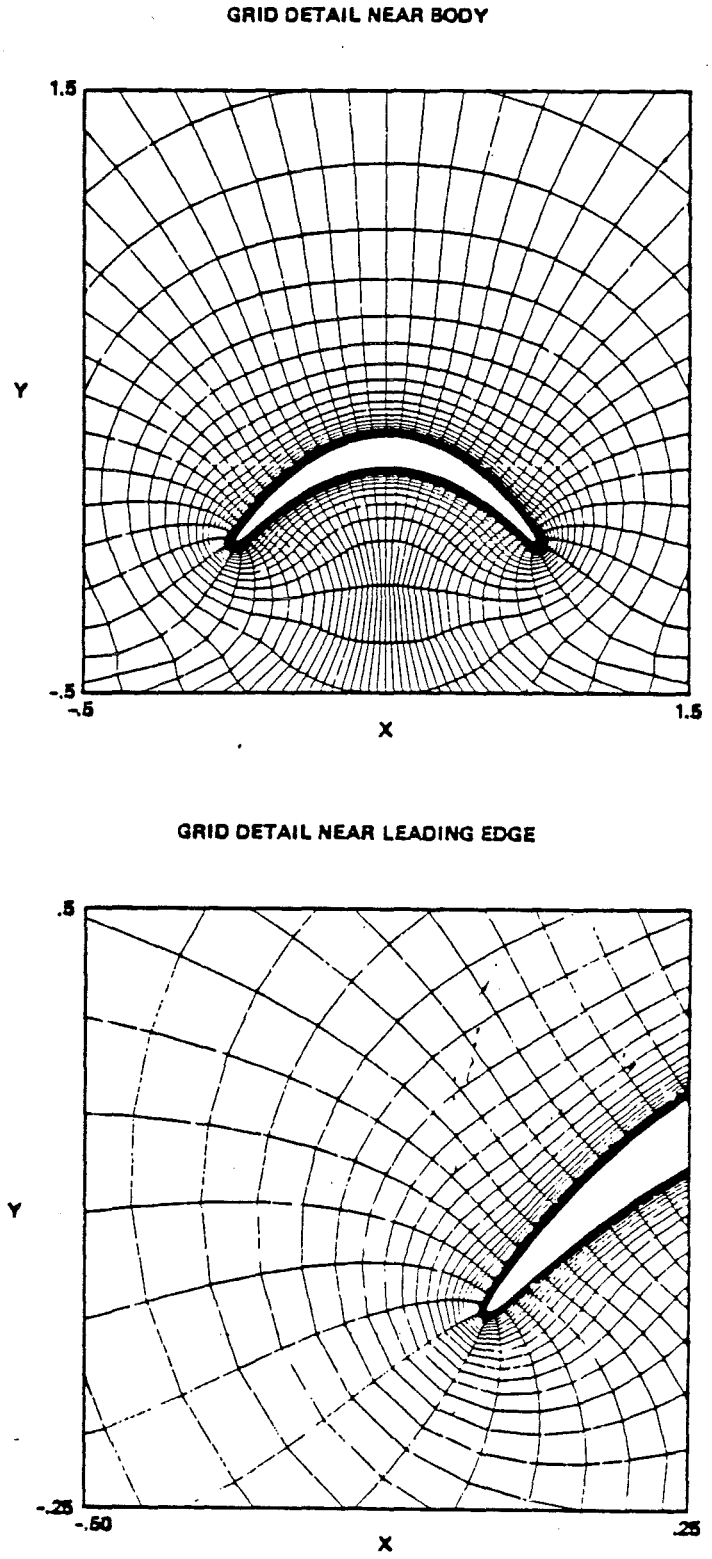

Figure 14. Viscous Grid Generated about Highly Cambered Airfoil

SECTION XV

FLUID DYNAMIC STABILITY

In a previous section we analyzed the stability of the numerical method. Criteria were established to insure that a stable algorithm was utilized in solving the fluid dynamic equations. The physical flows however can also exhibit an instability due to natural causes. It is the purpose of this section to identify the situation under which real instabilities can exist in order to help discern the difference from an unphysical numerical instability.

To demonstrate the procedure a common fluid dynamic instability will be investigated entitled the "Rayleigh Instability" (References 26 and 60).

Examine the incompressible, inviscid (Euler) equations.

$$U_x + V_y = 0$$

$$U_t + UU_x + VU_y = -P_x/\rho$$

$$V_t + UV_x + VV_y = -P_y/\rho$$

These last two equations may be combined to eliminate pressure by introducing vorticity.

$$\frac{D\underline{\omega}}{Dt} = 0$$

NOTE: $\omega \neq 0$
Rotational flow is considered here.

where

$$\underline{\omega} = \underline{\nabla} \times \underline{V} = (V_x - U_y)\,\underline{k}$$

1. PARALLEL FLOW

Assume that the flow can be represented as a disturbance from a steady-state parallel shear flow as follows:

$$U = \bar{U}(y) + U'(x,y,t)$$

$$V = 0 + V'(x,y,t)$$

Hence

$$\omega = Vx - Uy = (V'x - U'y) - \bar{U}y \equiv \omega' - \bar{U}y$$

The governing equations become

$$\nabla \cdot \underline{V} = U'x + V'y = 0$$

$$\frac{D\omega}{Dt} = \omega'_t + \bar{U}\omega'_x - \bar{U}_{yy}V' + (H.O.T.) = 0$$

The boundary conditions are that U' and V' vanish at $\pm \infty$.

The governing equations are linear and possess the following solution:

$$U' = \hat{U}(y)e^{i\alpha(x-ct)}$$

$$V' = \phi(y)e^{i\alpha(x-ct)}$$

where

$\hat{U}, \phi$ and c are complex

α = real (wave number)

Therefore

$$i\alpha\hat{U} + \phi_y = 0$$

$$\omega' = (i\alpha\phi - \hat{U}_y)e^{i\alpha(x-ct)}$$

$$(\bar{U} - C)(i\alpha\hat{U}_y + \alpha^2\phi) + \bar{U}_{yy}\phi = 0$$

Eliminating $\hat{U}$ produces the Rayleigh Equation.

$$\phi_{yy} - (\alpha^2 + \frac{\bar{U}_{yy}}{\bar{U} - C})\phi = 0$$

with boundary condition

$$\phi(\pm\infty) = 0$$

Given $\bar{U}$ and α these boundary conditions can only be achieved for specific values of $C = Cr + iCi$. This eigenvalue equation was first studied by Rayleigh in 1880. He derived a simple criterion for the condition under-which the flow was unstable, i.e. $Ci > 0$

2. CONDITION FOR INSTABILITY

Multiply the Rayleigh equation by the conjugate of ϕ (denoted by ϕ^*) and integrate over the entire domain.

$$\int_{-\infty}^{\infty}\left[\phi''\phi^* - \alpha^2\phi\phi^* - \frac{\bar{U}''}{\bar{U}-C}\phi\phi^*\right]dy = 0$$

Manipulating the terms to obtain the real and imaginary parts produce the following.

$$\int_{-\infty}^{\infty}\left[(\phi'\phi^*)' - \phi'\phi'^* - \alpha^2\phi\phi^* - \frac{\bar{U}''(\bar{U}-C^*)\phi\phi^*}{(\bar{U}-C)(\bar{U}-C^*)}\right]dy = 0$$

Since the first term vanishes due to boundary conditions

$$\int_{-\infty}^{\infty}(\phi'\phi^*)'dy = (\phi'\phi^*)_{-\infty}^{\infty} = 0$$

and the second and third terms are real, only the last term contains any imaginary part.

Hence

$$iC_i\int_{-\infty}^{\infty}\frac{\bar{U}''\phi\phi^*}{(\bar{U}-Cr)^2+C_i^2}dy = 0$$

This relationship can be satisfied in two ways, i.e. either $Ci = 0$ or $\bar{U}'' = 0$ somewhere. The later is the essential condition for an instability. This implies that the velocity profile exhibits an inflection point. This deduction is entitled Rayleigh's Second Theorem.

By inserting a value for $\overline{U} = \overline{U}(y)$ into the Rayleigh equation, eigenvalues for $C = C(\alpha)$ can be determined. This was accomplished by Verma, Hankey and Scherr (Reference 61) for the series of separated boundary layer profiles obtained from the Lower Branch solution of the Falkner-Skan equations. A plot of these results indicate that all the velocity profiles with inflection points are unstable (as indicated by Rayleigh's second theorem), however, only for a small range of frequency $\alpha\delta = \frac{\omega\delta}{Cr}$. In addition, large values of Ci are evident indicating a severe instability will occur.

SECTION XVII

TURBULENCE MODELS

Although turbulence is a self-excited oscillation and predictable using the Navier-Stokes equations, the scale of the smallest eddy would require extremely small grid sizes, thereby rendering the computation impractical. As a consequence, turbulence is treated as a fluid property and empirically added to the equations. In this section we will develop this concept.

Beginning with the two-dimensional, unsteady, incompressible Navier-Stokes equations we shall derive the Reynolds-averaged equations (Reference 26):

$$U_t + E_x + F_y = 0$$

$$U = \begin{vmatrix} o \\ u \\ v \end{vmatrix}; \quad E = \begin{vmatrix} u \\ u^2 - \sigma_{11}/\rho \\ uv - \tau/\rho \end{vmatrix}; \quad F = \begin{vmatrix} v \\ uv - \tau/\rho \\ v^2 - \sigma_{22}/\rho \end{vmatrix}$$

These variables are considered to be fluctuating in time about a well defined mean.

$$u = \bar{u}(x,y) + u'(x,y,t)$$
$$v = \bar{v}(x,y) + v'(x,y,t)$$
$$p = \bar{p}(x,y) + p'(x,y,t)$$

where

$$\bar{u} = \frac{1}{P}\int_t^{t+P} u\,dt$$

and

$$\int_t^{t+P} u'\,dt = 0$$

where the period over which the average is accomplished is large compared to the period for the lowest frequency component of concern.

$$\frac{1}{P} << f\,\text{min}\,(\sim 10\,\text{Hz for example})$$

Integrating and determining the mean produces the following:

$$\frac{1}{P}\int_t^{t+P}(U_t + E_x + F_y)\,dt = 0$$

The linear terms (u, v, p, τ_{ij}, σ_{ii}), merely produce the mean values. The non-linear terms produce additional terms.

$$\frac{1}{P}\int_t^{t+P} u^2 dt = \frac{1}{P}\int_t^{t+P}(\bar{u}^2 + 2\bar{u}u' + u'^2)\,dt = \bar{u}^2 + \overline{u'^2}$$

similarly

$$\frac{1}{P}\int_t^{t+P} v^2 dt = \bar{v}^2 + \overline{v'^2}$$

$$\frac{1}{P}\int^{t+P} uv\,dt = \bar{u}\bar{v} + \overline{u'v'}$$

Therefore

$$U = \begin{vmatrix} 0 \\ \bar{u} \\ \bar{v} \end{vmatrix};\quad E = \begin{vmatrix} \bar{u} \\ \bar{u}^2 + \overline{u'^2} - \overline{\sigma 11/\rho} \\ \bar{u}\bar{v} + \overline{u'v'} - \bar{\tau}/\rho \end{vmatrix};\quad F = \begin{vmatrix} \bar{v} \\ \bar{u}\bar{v} + \overline{u'v'} - \bar{\sigma}/\rho \\ \bar{v}^2 + \overline{v'^2} - \bar{\sigma}_{22}/\rho \end{vmatrix}$$

The additional terms all appear next to one of the stress terms. These new terms are entitled "apparent stresses" or Reynolds stresses. It is therefore convenient to redefine these stresses for turbulent flow to make the equations identical in form to the laminar equations.

$$\tau_{11_{turb}} = -\bar{p} + \lambda\nabla\cdot\bar{\underline{v}} + 2\mu\bar{u}_x - \rho\overline{u'^2}$$

$$\tau_{12_{turb}} = \mu(\bar{u}y + \bar{v}x) - \rho\overline{u'v'}$$

$$\tau_{22_{turb}} = -\bar{p} + \lambda\nabla\cdot\bar{\underline{v}} + 2\mu\bar{v}y - \rho\overline{v'^2}$$

By analogy with the description of viscous stresses created by the molecular viscosity, we can define a turbulent (or eddy) viscosity as follows:

$$-\rho\overline{u'v'} \equiv \epsilon_{12}(\bar{u}y+\bar{v}x)$$
$$-\rho\overline{u'^2} \equiv \epsilon_{11}(-2/3\nabla\cdot\bar{\underline{v}}+2\bar{u}_x)$$
$$-\rho\overline{v'^2} \equiv \epsilon_{22}(-2/3\nabla\cdot\bar{\underline{v}}+2\bar{v}y)$$

It can be shown that ϵ is always positive defined in this manner to prevent violation of the second law of thermodynamics. Since insufficient empirical information is available to evaluate these different eddy viscosity coefficients they are equated to each other. The largest term of engineering importance is $\varepsilon_{12}\,\bar{U}_y$ and requires the greatest attention. The remaining terms generally contribute little and need not be evaluated accurately.

Therefore $$\epsilon = \epsilon_{12} = \epsilon_{11} = \epsilon_{22}$$

The magnitude of the apparent stresses overwhelms the molecular viscosity terms (except on the surface) since

$$\frac{\epsilon}{\mu} \sim 100 \text{ to } 1000 \text{ for } 10^6 < Re < 10^8$$

Therefore, the Reynolds-averaged equations are obtained simply by replacing μ by ε in all stress terms.

For compressible flow we include the density fluctuations and the energy equation, i.e., $\rho = \bar{\rho} + \rho'$

However, it can be shown that the ρ' variation produces little change in the equations up to M=5. This is due in part to the fact that the U' disturbance is still subsonic up to $\bar{M} \approx 5$. In the energy equation the thermal conductivity is replaced by the turbulent conductivity.

$$K = K_t$$

which is evaluated by means of the eddy viscosity, ε, and turbulent Prandtl number.

$$Pr_{lam} = \frac{\mu Cp}{K} = 0.72$$

$$Pr_{turb} = \frac{\epsilon Cp}{K_t} \cong 1.0$$

Therefore, the compressible, turbulent Reynolds-averaged equations are identical to the compressible laminar Navier-Stokes equations with new values for the transport properties.

1. EVALUATION OF EDDY VISCOSITY

Thus, there is no difference between calculating laminar or turbulent flow except for the calculation of ε. In this section, we will examine simple turbulence models (Reference 62). Although complex relationships involving a system of partial differential equations with 27 unknown coefficient have been derived to evaluate the Reynolds-stresses, they have not produced as originally advertised. The present method in vogue today is to use simple algebraic models and adjust the constants for the special cases under consideration. Hopefully, a pattern will evolve as more experimental data and numerical comparisons are produced.

2. BOUSSINESQ MODEL

By forming a dimensionless turbulent, Reynold's number for turbulent boundary layers a correlation was determined.

$$Re_{turb} = \frac{\rho U_e \delta}{\epsilon} = 60$$

3. CLAUSER LAW OF THE WAKE

It was later found that using the incompressible displacement thickness, δ_i^*, for the length scale, the outer 80% wake-like region of compressible turbulent boundary layers could be correlated.

$$\epsilon_{outer} = K_2 \rho U_e \delta i^*$$

where $K_2 = (60)^{-1} = .0168$

and $\delta i^* = \int_o^\infty (1 - \frac{U}{U_e}) dy$

4. VON-KARMAN LAW OF THE WALL

In the inner 20% ε diminishes from the above value due to the presence of the wall.

Experiments indicated a logarithmic velocity variation near the wall from which the eddy viscosity could be deduced.

$$\epsilon = \rho (K_1 y)^2 \left| \frac{du}{dy} \right| \text{ where } K_1 = 0.4$$

The shear stress is nearly constant in the vicinity of the wall for zero longitudinal pressure gradient (flat plate).

$$\left. \frac{\partial \tau}{\partial y} \right|_o = \left. \frac{dp}{dx} \right|_o = 0$$

$$\text{Therefore } \tau = \tau_w = \epsilon \frac{du}{dy}$$

$$\text{or } \frac{\tau_w}{\rho} = (K_1 y \frac{du}{dy})^2 \equiv U^{*2}$$

Integrating this expression reaffirms the logarithmic velocity profile variation.

$$\frac{U}{U^*} = \frac{1}{K_1} \ln \frac{y u^*}{\nu} + C_1$$

Experiments show that C=5 for smooth flat plates.

5. VAN DRIEST DAMPING FACTOR

Refined measurements near the wall identified the existence of a laminar sublayer. Van Driest developed an expression to join the laminar region to the law of the wall region.

The following damping factor, D, was inserted into the length scale.

$$D = 1 - e^{\frac{-yU^*}{\nu A}}$$

$$\text{where } A = 26$$

The inner value for the eddy viscosity becomes the following:

$$\epsilon_{inner} = \rho (K_1 y D)^2 \left| \frac{du}{dy} \right|$$

6. CEBECI-SMITH MODEL

A combination of the above relations is called the Cebesci-Smith Model. A two-layer turbulence model is used for the inner and outer eddy viscosity. Both are programmed and computed separately, however, the lesser value of the two is used in each region.

7. BALDWIN-LOMAX MODEL

Since the two-layer model is somewhat awkward in joining two separate functions, a unified method is preferred. In addition, relating the turbulence to vorticity is regarded as fundamental by some investigators. The Baldwin-Lomax model accomplishes these features.

$$\epsilon = \rho (Dl)^2 |\omega|$$

$$\text{where } l = .08\delta \tanh\left(\frac{.41y}{.08\delta}\right)$$

8. FAR WAKE MODEL

For far wakes the form of the law of the wake is used, however, the coefficient increases by a factor of 4.

$$\epsilon_{wake} = .064 \rho U_e \delta_i^*$$

Empirical correlations are used to join ε in the various regions of the flowfield.

SECTION XVIII

SUMMARY

Included herein is an introduction to Computational Aerodynamics in which the major topics are addressed. The purpose of this report is to provide a foundation for those just entering the field. It is intended that additional sections be added in the future as further developments evolve in the subject area.

REFERENCES

1. Granger, R., Incompressible Fluid Dynamics, United States Naval Academy, 1975.

2. Kopal, Z., Tables of Supersonic Flow Around Cones, MIT Cambridge, Mass., 1947.

3. Blottner, F., "Finite Difference Methods for Solution of the Boundary Layer Equations", AIAA Journal, Vol. 8, No. 2, February 1970.

4. MacCormack, R., "Numerical Solution of the Interaction of a Shock Wave with a Laminar Boundary Layer," Lecture Notes in Physics, Vol. 8, Springer Verlag, New York, 1971.

5. Lomax, H., "Recent Progress in Numerical Techniques for Flow Simulation," AIAA Journal, Vol. 14, No. 4, 1976.

6. Calahan, D., "Performance of Linear Algebra Codes on the CRAY-1", Proceedings SPE Symposium on Reservoir Simulation, Denver, Colorado, 1979.

7. Rutherford, A., Vectors, Tensors and the Basic Equations of Fluid Mechanics, Prentice-Hall, 1962.

8. Leipmann, H. and Roshko, A., "Elements of Gas Dynamics", J. Wiley and Sons, Inc., 1957.

9. Hughes, W., Gaylord, E., Basic Equations of Engineering Science, Schaum's Outline Series, McGraw-Hill Book Co., 1964.

10. Vivand, H., "Conservative Forms of Gas Dynamics Equations," LaReclerche Aerospatile, No. 1, January 1974.

11. Vinokur, M., "Conservative Equations of Gas Dynamics in Curvilinear Coordinate Systems", Journal of Comp. Physics, Vol. 14, February 1974.

12. Peyret, R. and Vivand, H., "Computation of Viscous Compressible Flows Based on the Navier-Stokes Equations," AGARDograph No. 212, September 1975.

13. Cheng, S.I., "A Critical Review of the Numerical Solution of the Navier-Stokes Equation," Lecture Notes in Physics Springer Verlog, Berlin, 1974.

14. Shang, J. and Hankey, W., "Numerical Solution for Supersonic Turbulent Flow Over a Compression Ramp," AIAA Journal, Vol. 13, No. 10, October 1975.

15. Shang, J., Hankey, W., and Law C., "Numerical Simulation of Shock-Wave Turbulent Boundary Layer Interactions", AIAA Journal, Vol. 14, No. 10, October 1976.

REFERENCES (Cont'd)

16. Shang, J. Hankey, W., "Numerical Solution of the Navier-Stokes Equations for a Three-Dimensional Corner", AIAA Journal, Vol. 15, No. 11, November 1977.

17. Hung, C., MacCormack, R., "Numerical Solution of Supersonic Laminar Flow Over a Three-Dimensional Compression Corner", AIAA paper, 77-694, 1977.

18. Briley, W., "A Numerical Study of Laminar Separation Bubbles Using the Navier-Stokes Equations," Journal of Fluid Mechanics, Vol. 47, Part 4, 1971.

19. Knight, D., "Numerical Simulation of Realistic High-Speed Inlets Using the Navier-Stokes Equations", AIAA Journal, Vol. 15, No. 11, November 1977.

20. Roache, P., and Meuller, T., "Numerical Solutions of Laminar Separated Flows", AIAA Journal, Vol. 8, No. 3, 1979.

21. McRae, D., "A Numerical Study of Supersonic Viscous Cone Flow at High Angles of Attack," AIAA Paper 76-97, January 1976.

22. Schiff, L., and Steger, J., "Numerical Simulation of Steady Supersonic Viscous Flow", AIAA Preprint 79-0130, January 1979.

23. El-Mistikawy T., and Werle, M., "Numerical Methods for Inviscid/ Viscous Fluid Flows", Rept. No. AFL 77-9-34, Dept. of Aerospace Engineering, University of Cincinnati, September 1977.

24. Kutler, P., "Numerical Solutions for Inviscid Supersonic Flow in the Corner Formed by Two Intersecting Wedges", AIAA Paper 73-675, 1973.

25. Van Dyke, M., "A Study of Hypersonic Small Disturbance Theory," NACA Rept. 1194, 1954.

26. Schlichting, H., Boundary Layer Theory, McGraw-Hill Book Co., Inc. New York, 1968.

27. Davis, R., "Numerical Solution of the Hypersonic Viscous Shock-Layer Equations," AIAA Journal, Vol. 8, No. 5, May 1970.

28. Richtmyer, R., "A Survey of Difference Methods for Non-Steady Fluid Dynamics", NCAR Tech Notes 63-2, Boulder, Colorado, 1963.

29. Carnahan, B., Luther, H., and Wilke, J., "Applied Numerical Methods," J. Wiley and Sons, Inc., New York, 1969.

30. Hankey, W., and Holden, M., "Two-Dimensional Shock Wave Boundary Layer Interactions in High Speed Flows", AGARD AG 203, June 1975.

REFERENCES (Cont'd)

31. Roache, P.J., "Computational Fluid Dynamics," Hermosa Publishers, Albuquerque, New Mexico, 1972.

32. Richtmyer, R. D., and Morton, K. W., "Difference Methods for Initial Valued Problems," Interscience Publisher, New York, 2nd Edition, 1967.

33. Keller, H., "Numerical Methods for Two-Point Boundary Value Problems", Blaisdel Publishing Co., 1968.

34. Forsythe, W., "Finite-difference Methods for Partial Differential Equations," J. Wiley and Sons, Inc. New York, 1960.

35. Lilly, D., "On the Computational Stability of Numerical Solutions of Time Dependent Nonlinear Geophysical Fluid Dynamics Problems" U.S. Weather Bureau Monthly Weather Review, Vol. 93, No. 1, 1965.

36. Dufort, E. and Frankel, S., "Stability Conditions in the Numerical Treatment of Parabolic Differential Equations," Math Tables and Other Aids to Computation, Vol. 7, 1953.

37. Taylor, P., "The Stability of the Dufort Frankel Method for the Diffusion Equation with Boundary Conditions, Involving Space Derivatives,", The Computer Journal Vol. 13. No. 1, 1970.

38. Courant, R., Friedrichs, K. and Lewy, H. "Uberdie Partiellen Differenzeng leichurgen der Mathematichen Physik" Mathematische Annalen, Vol. 100, 1928.

39. Lax, P., and Wendroff, B., "Difference Schemes with High Order Accuracy for Solving Hyperbolic Equations" Communications on Pure and Applied Mathematics, Vol. 17, 1964.

40. Lax, P. and Wendroff, B., "System of Conservative Laws,", Comm. Pure Applied Math., Vol. 13, 1960.

41. Crank, J., and Nicolson, P., "A Practical Method for Numerical Integration of Solutions of Partial Differential Equations of Heat Conduction Type, Proc. Cambridge Philos, Vol. 43, 1947.

42. Beam R., and Warming R., "An Implicit Factored Scheme for Compressible Navier-Stokes Equations", AIAA Journal, Vol. 16, No. 4, April 1978.

43. Bird, R., Stewart, W., Lightfoot, E., Transport Phenomena, John Wiley & Sons, Inc., New York, 1960.

44. Ames Research Staff, Equations Tables and Charts for Compressible Flow, NA CA TR 1135, 1953.

REFERENCES (Cont'd)

45. Roache, P., "On Artificial Viscosity", Journal of Computational Physics, Vol. 10, No. 2, 1972.

46. Rusanov, V., "Calculation of Interaction of Non-Steady Shock Waves with Obstacles," Zhur Vschislitel Noi Mathematicheskoi, Fiziki, Vol. 1, No. 2, 1961.

47. Kreiss, H., "On Difference Approximations of the Dissipative Type for Hyperbolic Differential Equations," Comm. Pure Appl. Math., Vol. 17, 1964.

48. Hodge, J., "Numerical Solution of Incompressible Laminar Flow about Arbitrary Bodies in Body-Fitted Curvilinear Coordinates," Ph.D Thesis Mississippi State University, December 1975.

49. Hankey, W., Neumann, R., Flinn, E., Design Procedures for Computing Aerodynamic Heating at Hypersonic Speeds, WADCTR 49-610, June 1960.

50. Moretti, G., "The Importance of Boundary Conditions in the Numerical Treatment of Hyperbolic Equations," Polytech Institute of Brooklyn PIBAL Rept. No. 68-34, November 1968.

51. Morse, P., and Feshback, H., Methods of Theoretical Physics, Part I, McGraw-Hill Book Co., Inc., New York, 1953.

52. Sommerfeld, A. "Partial Differential Equations in Physics," Academic Press, Inc. New York, 1949.

53. Hadamand, J., "Lecture on Couchy's Problem in Linear Partial Differential Equations,", Yale University Press, New Haven, Connecticut, 1923.

54. Christian, J., Hankey, W., and Petty, J., "Similar Solutions of the Attached and Separated Compressible Laminar Boundary Layer with Heat Transfer and Pressure Gradient," USAF, ARL 70-0023, February 1970.

55. McKenna, J., Hankey, W., and Graham, J., "Implementation of the Characteristic Variables as Boundary Conditions for the Navier-Stokes Equations," To be published as AFWAL TR.

56. Smith, R., Numerical Grid Generation Techniques, NASA CP2166, October 1980.

57. Thompson, J., Thames, F., and Mastin, C., "Automatic Numerical Generation of Body-Fitted Curvilinear Coordinate System for Field Containing Any Number of Arbitrary Two-Dimensional Bodies," Journal Computational Physics, Vol. 15, No. 3, July 1974.

REFERENCES (Cont'd)

58. Douglas, J., "On the Numerical Integration by Implicit Methods," J. Sec. Industrial and Appl. Math., Vol. 3, 1955.

59. Douglas, J., Gunn, J., "A General Formulation of Alternating Direction Methods, I." Numer Math., Vol. 6, 1964.

60. Lees, L., Lin C., "Investigation of the Stability of the Laminar Boundary Layer in a Compressible Fluid," NACATN No. 1115, 1946.

61. Verma, G. Hankey, W. and Scherr, S. "Stability Analysis of the Lower Branch Solutions of the Falkner-Skan Equations" AFFDL-TR-79-3116, July 1979.

62. Shang, J., Hankey, W. and Dwoyer, D., "Numerical Analysis of Eddy Viscosity Models in Supersonic Turbulent Boundary Layers," AIAA Journal, Vol. 11, No. 12, December 1973.

*USGPO: 1983-659-062-1012